Marine and Petroleum Geology 77 (2016) 323–340

Contents lists available at ScienceDirect

Marine and Petroleum Geology

journal homepage: www.elsevier.com/locate/marpetgeo

Research paper

New insights about petroleum geology and exploration of Qiangtang Basin, northern Tibet, China: A model for low-degree exploration

Xiugen Fu [a, b, *], Jian Wang [a, b], Fuwen Tan [a, b], Ming Chen [a], Zhongxiong Li [a], Yuhong Zeng [a, b], Xinglei Feng [b]

[a] Chengdu Institute of Geology and Mineral Resources, Chengdu 610081, China
[b] Key Laboratory for Sedimentary Basin and Oil and Gas Resources, Ministry of Land and Resources, Chengdu 610081, China

ARTICLE INFO

Article history:
Received 11 September 2015
Received in revised form
1 June 2016
Accepted 16 June 2016
Available online 18 June 2016

Keywords:
Petroleum geology
Sedimentary characteristics
Favorable exploration area
Exploration potential
Qiangtang Basin

ABSTRACT

The Qiangtang Basin is the biggest petroleum-bearing basin in the Qinghai-Tibet Plateau. This basin experienced a foreland basin evolution during the Early- Middle Triassic and a rift basin evolution during the Late Triassic-Early Cretaceous. Triassic and Jurassic hydrocarbon source rocks were widely distributed throughout the basin. The Triassic Tumen Gela Formation coal-bearing mudstones represent the best source rocks because of high total organic carbon (TOC) content (1.25–3.45%) and HI values (2.8–123 mg/g Toc), and the Xiali Formation mudstones are moderately-good source rocks with an average TOC content ranging from 0.55 to 7.30% and HI values ranging from 7.0 to 165 mg/g Toc. The Jurassic Buqu Formation and Suowa Formation carbonates, however, exhibit poor-to fair-quality as hydrocarbon source rocks. Excellent dolomite and paleokarst reservoirs and mudstones and bearing-evaporite marl cap rocks, together with well-developed structural traps are recognized in the basin. Additionally, a large paleo-oil-reservoir zone has also been discovered.

Based on an integrated petroleum systems analysis, nine favorable hydrocarbon exploration areas are proposed, of which the Tuonamu area and Badaohu area are selected as the potential targets for the exploration for oil and gas resources in the basin. Good reservoir quality dolomites in the Buqu Formation are considered to have a significant exploration potential.

1. Introduction

The Qinghai-Tibet Plateau, covering an area about 2.6×10^6 km^2 (Xiong et al., 2009), is located in the middle part of the Tethyan tectonic domain within which concentrates over two-thirds of global petroleum reserves (Klemme and Ulmishek, 1991). More than twenty marine basins and sixty-eight continental basins have been found in this region, of which the Qiangtang Basin is the largest (about 220×10^3 km^2), with favorable conditions for petroleum generation and entrapment (Zhao and Li., 2000).

The exploration history of the Qinghai-Tibet Plateau started in the 1950s. The main drilling activities were concentrated in the Lunpola Basin, where two small oil fields had been discovered from the 1960s–1980s. Since 1993, large-scale oil and gas reconnaissance and exploration have been carried out in the Qiangtang Basin by PetroChina (Zhao and Li., 2000). In 2001, new oil and gas reconnaissance and exploration actives were undertaken by the Chengdu Institute of Geology and Mineral Resources. According to the regional survey for oil and gas, more than 200 surface oil and gas shows have been found in Mesozoic formations (Wang et al., 2004b; Fu et al., 2008; Zeng et al., 2013). However, the exploration level of oil and gas in the Qinghai-Tibet Plateau is the lowest in China due to complicated tectonic evolution (Kapp et al., 2003; Yin and Harrison, 2000) and poor natural environmental conditions (e.g., extreme altitude, lower levels of oxygen, and severe climatic conditions).

In recent years, updated analytical techniques and concepts, such as seismic stratigraphy and petroleum system studies, were applied to more fully evaluate the hydrocarbon exploration potential of the Qiangtang Basin. A large paleo-oil-reservoir zone was discovered in the basin (Wang et al., 2004b), and gas show was also found by mud volcano investigation (Fu et al., 2013). Our new data also reveal that thick Mesozoic marine sediments were well developed in the Qiangtang Basin, and a total thickness of Paleozoic

* Corresponding author. Chengdu Institute of Geology and Mineral Resources, Chengdu 610081, China.
E-mail address: fuxiugen@126.com (X. Fu).

http://dx.doi.org/10.1016/j.marpetgeo.2016.06.015
0264-8172/

(6500 m), Mesozoic (6000 m), and Cenozoic (1500 m) strata is more than 13, 000 m (Wang et al., 2009). The Qiangtang Basin, therefore, is an area of potential future exploration, and oil and gas exploration will likely intensify in the near future.

In the present study, we integrate previous research with new data obtained from outcrop and subsurface studies including 1430 samples, 735 km seismic lines, and 12 shallow wells (Fig. 1b) to: (1) summarize the petroleum geology of the Qiangtang Basin; (2) proposes nine favorable hydrocarbon exploration areas and two key targets for the future; and (3) discuses the exploration potential of the basin.

2. Geologic settings

2.1. Tectonic evolution

From north to south, the Tibetan plateau consists of the Kunlun-Qaidam terrane, Songpan-Ganzi flysch complex, Qiangtang and Lhasa terranes, which are separated by the Hoh Xil-Jinsha River and Bangong Lake-Nujiang River suture zones, respectively (Fig. 1a). It is generally accepted that the Paleo-Tethys, represented at the present-day by the Hoh Xil-Jinsha River suture, opened probably in the Early Carboniferous time and was closed by the Permian to Late Triassic time (Dewey et al., 1988; Pearce and Mei, 1988; Nie et al., 1994; Kapp et al., 2003; Zhang et al., 2013). The Meso-Tethyan seaway between the Lhasa and Qiangtang terranes was open by the Late Triassci to Early Jurassic time and closed along the Bangong Lake-Nujiang River suture during the Late Jurassic time (Pearce and Mei, 1988; Yin and Harrison, 2000; Kapp et al., 2003; Wang et al., 2009; Liang et al., 2012).

The Qiangtang terrane, bounded by the Bangong Lake-Nujiang River suture zone to the south and the Hoh Xil-Jinsha River suture zone to the north, respectively, consists of the North Qiangtang depression, the Central uplift and the South Qiangtang depression (Figs. 1b and 2). It is considered to have undergone a two-stage evolution during the Mesozoic time, i.e., the Early-Middle Triassic evolution and the Late Triassic (or late middle Triassic)-Early Cretaceous evolution (Fig. 3). According to the study by Wang et al. (2004a, 2009), the Qiangtang Basin experienced a foreland basin evolution during the Early- Middle Triassic. In this interval, the South Qiangtang depression and Central uplift were uplifted entirely (Wang et al., 2004a), whereas the North Qiangtang depression was still a depositional area. During the Late Triassic (ca. 220–201 Ma), large-scale volcanic-eruption and volcanic-sedimentary events took place in the Qiangtang Basin, indicating a new history of tectonic and sedimentary evolution (i.e. rifting evolution, Fu et al., 2010a).

2.2. Stratigraphic and sedimentary characteristics

The early sedimentary successions of the Mesozoic Qiangtang Basin consist of alluvial and fluvial volcanoclastic deposits associated with continental explosive volcanic facies of the Nadi Kangri Formation (Wang et al., 2004a; Fu et al., 2010a), which are overlain by littoral to shallow-marine facies. Subsequently, a carbonate-platform facies association developed as a result of rapid differential subsidence and the consequent sea-level rise and transgression (Fu et al., 2010a). Therefore, the early sedimentary history of the Mesozoic Qiangtang Basin is characterized by a progradational sequence of transition from continental to marine facies, suggesting a progressive rift extension (Fu et al., 2010a).

2.2.1. The upper Triassic Nadi Kangri and Tumen Gela Formations

The Late Triassic Nadi Kangri volcanic rocks, with nearly east-west trending outcrops within the Qiangtang Basin along the northern Tibet, China, are composed largely of acidic tuff, dacite, rhyolite and minor basic volcanic rocks with a thickness of 217 to 1571 m (Fig. 4). The pre-Nadi Kangri paleo-weathered crusts are overlain unconformably by the Nadi Kangri volcanic rocks (Fu et al., 2010a). Therefore, the Nadi Kangri volcanic rocks represent the beginning of Mesozoic fill of the basin. These volcanic rocks are dated at the Late Triassic (about 205–220 Ma) (Fu et al., 2010a). In this interval, the explosive center was located in the northern and southern parts of the North Qiangtang depression (Fig. 5), where are continental-margin near-shore lacustrine deposits (Wang et al., 2004a) (Fig. 5). Sedimentary structures such as flow and

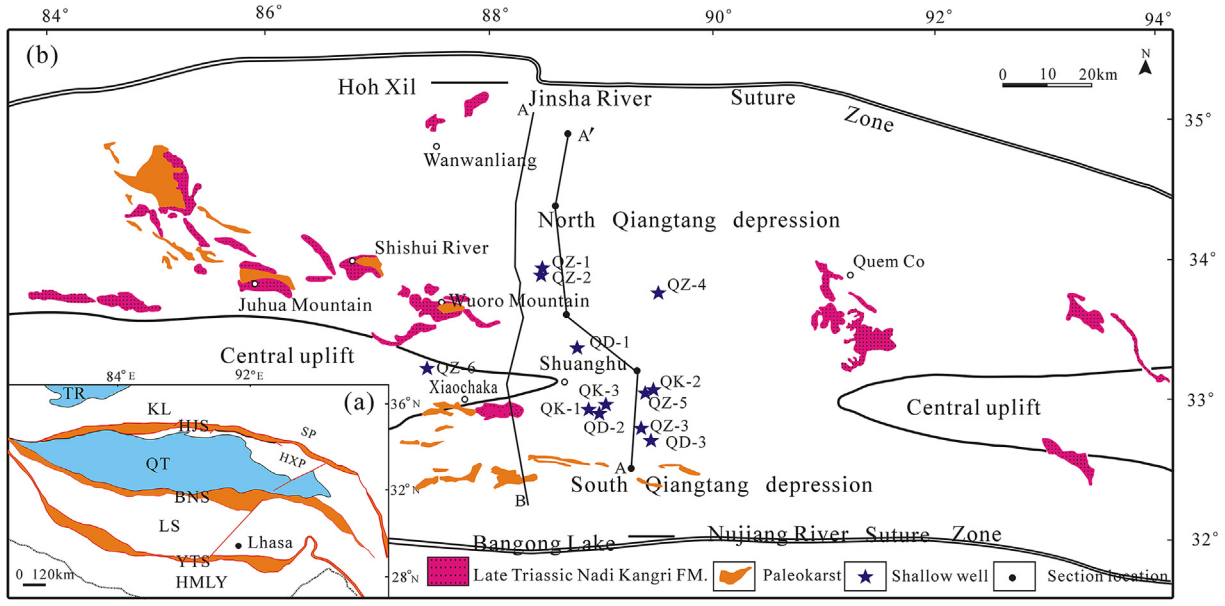

Fig. 1. (a) Map of the Tibetan plateau showing major Terranes. (b) Simplified tectonic map of the Qiangtang Basin, showing wells, main seismic lines, major structural elements, and late Triassic strata and paleokarst (modified from Fu et al., 2010a, b). TR-Tarim Basin; KL-Kunlun terrane; SP-Songpan-Ganzi flysch complex; HJS- Hoh Xil-Jinsha River suture; HXP-Hoh Xili piedmont zone; QT-Qiagtang Basin; BNS– Bangong Lake-Nujiang River suture; LS-Lhasa terrane; YTS–Yarlung Tsangpo suture; HMLY-Himalayas.

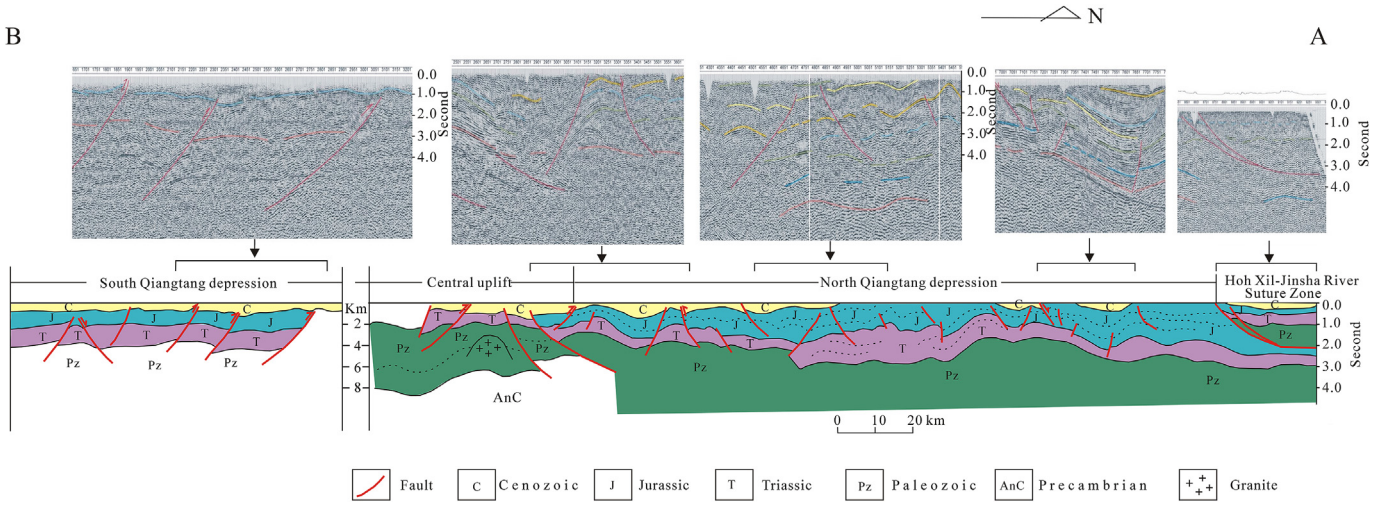

Fig. 2. Schematic cross section (the location is in Fig. 1) across the Qiangtang Basin (modified from Wang et al., 2009). The line of the section is shown in Fig. 1b.

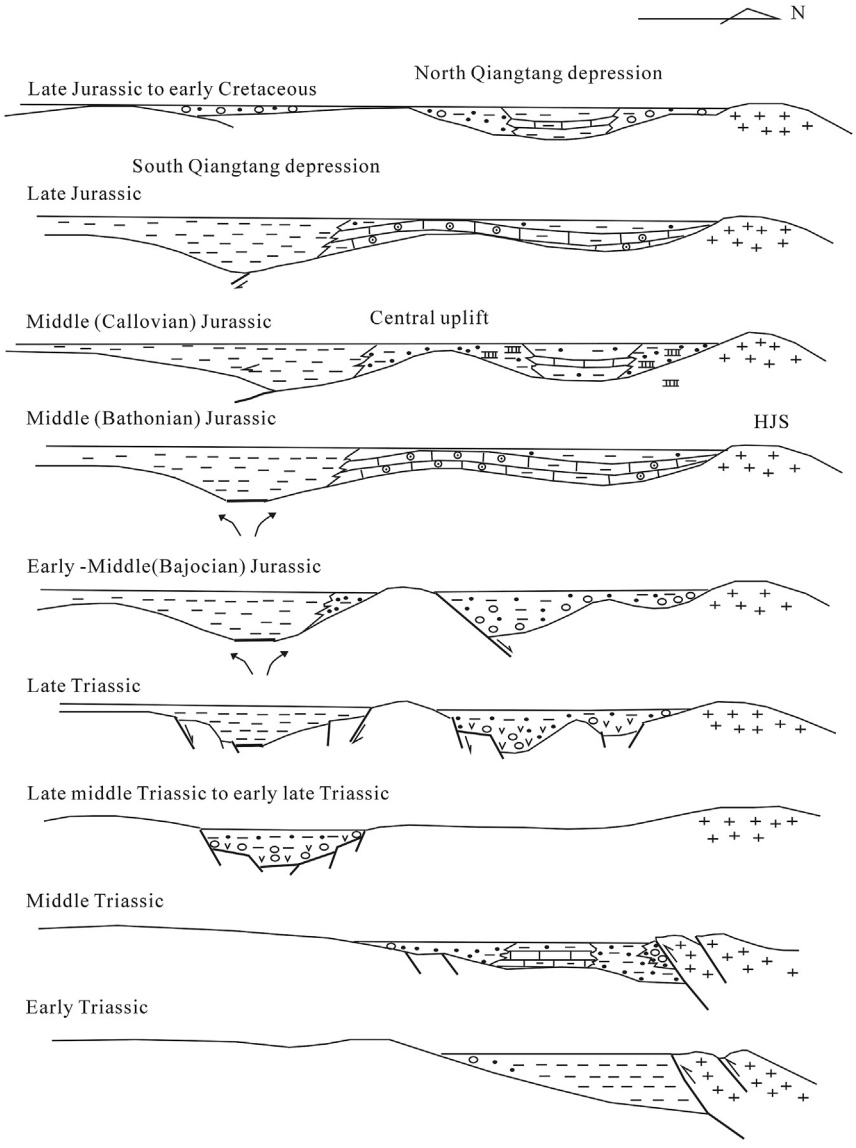

Fig. 3. Two-stage model of the Mesozoic tectonic evolution of the Qiangtang Basin (modified from Wang et al., 2004a; the legends are the same as in Fig. 4).

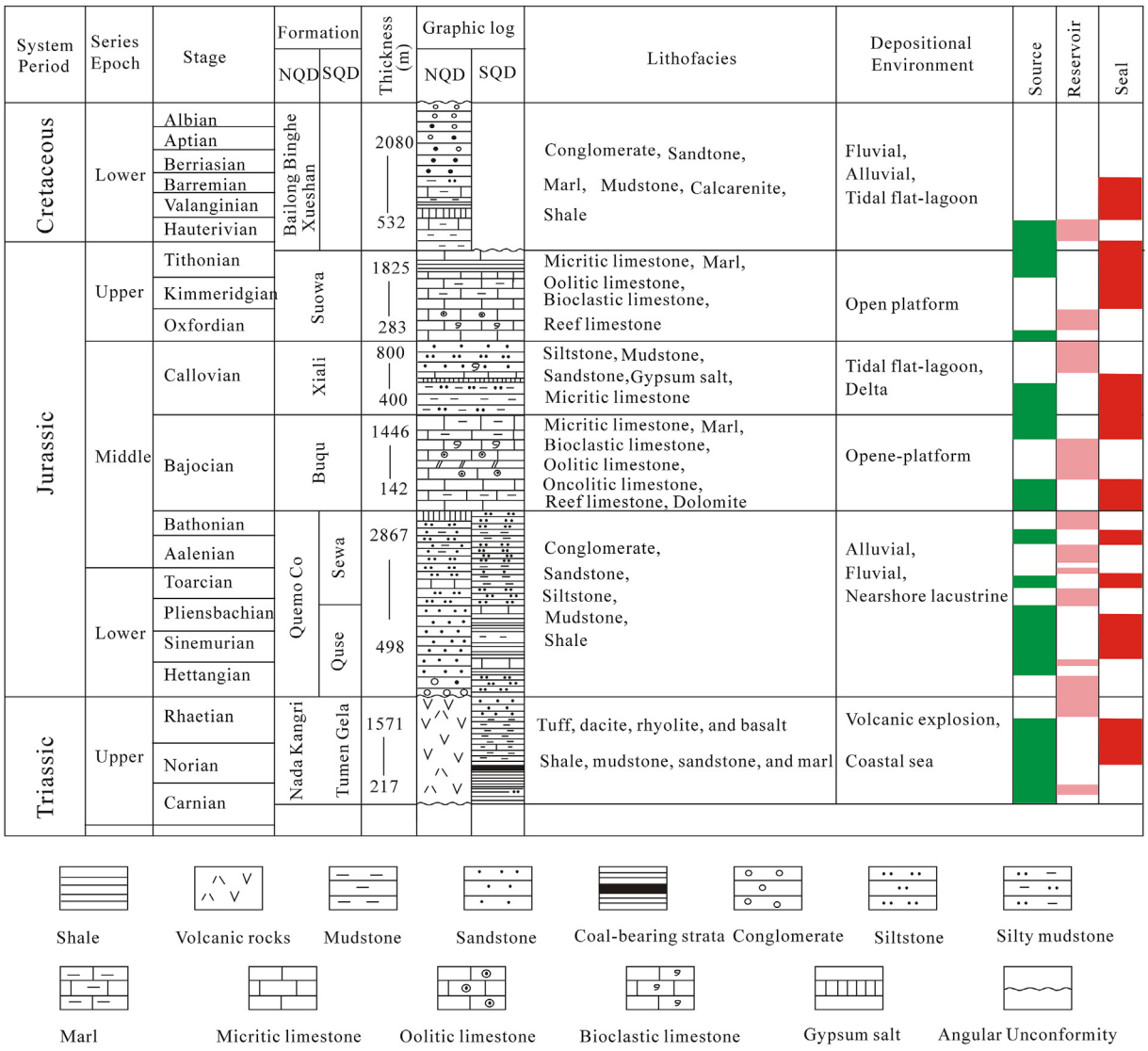

Fig. 4. A schematic diagram showing major stratigraphic units, and petroleum and sedimentary characteristics of the Qiangtang Basin (modified from Zeng et al., 2013). NQD-North Qiangtang depression; SQD-South Qiangtang depression.

amygdaloidal structures and porphyritic texture were well developed, indicating the explosive or effusive eruption facies environment.

The Tumen Gela Formation consists largely of shale, mudstone, sandstone, and marl intercalated with coal (Fig. 4). This unit is spread mainly along the margin of the basin with a thickness ranging from several hundred meters to 1000 m (some places up to 3000 m). The mudstone, marl interbedded coals occur mainly along the margin of the basin, and represent deposition in coastal swamp environments. The shallow-marine shale and sandstone were widely developed in the northern part of the basin (Zeng et al., 2013). Our new well data reveal that the shelf facies shale is widespread in the central part of the eastern Qiangtang Basin. According to the fossils found including bivalve associations (e.g., *Halobia* sp., *Palaeocardita sp.*, *Entolium sp.*), corals (e.g., *Margarophyllum decora* Wu), and plant fossils (e.g., *Equisetites* cf. *fergansensis* Soward) (Chengdu Institute of Geology and Mineral Resources, 2005b), the age of the Tumen Gela Formation is Late Triassic, and the lower part is possibly latest Middle Triassic.

2.2.2. *The early to middle Jurassic Quemo Co Formation and Sewa/Quse Formation*

The Quemo Co Formation is distributed mainly in the North Qiangtang depression with a thickness ranging from 498 to 1953 m (Fu et al., 2010b). This unit unconformably/disconformably overlies the Nadi Kangri Formation volcaniclastic rocks or Tumen Gela Formation stratum in the basin (Fu et al., 2010b). Abundant bivalves and spores and pollen grains, occurring at the top of the Quemo Co Formation (Fu et al., 2010b), indicate that the Quemo Co strata are of Early to Middle Jurassic age. The sediments, consisting of coarse-grained sandstone, fine-grained sandstone, siltstone, and mudstone intercalated with micritic limestone, marl and evaporitic rocks, display an overall upward-fining succession (Fig. 4). Some laterally discontinuous conglomeratic and coarse-sandstone beds at the base of the Quemo Co Formation represent initial fluvial and alluvial deposition (Wang et al., 2009). Purplish-red medium-bedded coarse sandstone, fine sandstone, and siltstone intercalated with micritic limestone constitute the lower and middle portions of the Quemo Co Formation. Sedimentary structures such as small-scale cross bedding, parallel bedding, mud cracks, and worm

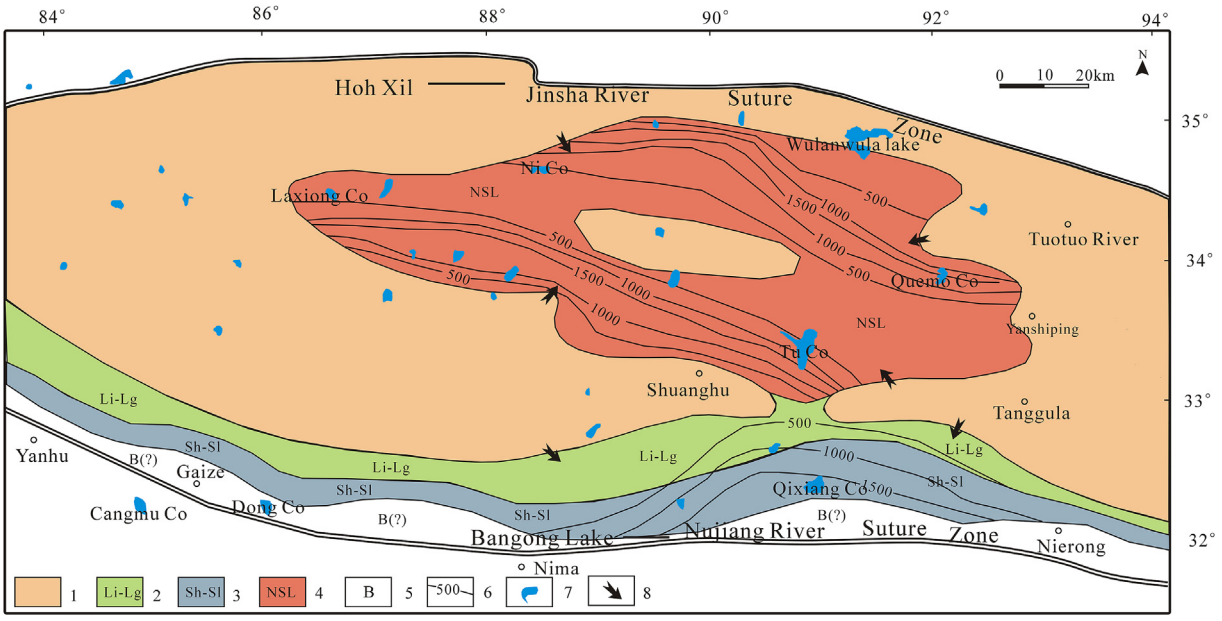

Fig. 5. Late Triassic paleogeographic and depositional environment maps of the Qiangtang Basin (modified from Wang et al., 2004a). 1, Erosion area; 2, Littoral-lagoon facies; 3, Shelf-slope facies; 4, Near-shore lacustrine; 5, Basin facies; 6, Thickness contour (m); 7, Lake; 8, Provenance.

burrows are observed as well salt, brackish, and fresh water bivalve fossils have been found (Wang et al., 2004a, b), representing a transgressive lacustrine environment (Fig. 6). The upper part of the Quemo Co Formation consists of gray-colored thin-bedded mudstone and siltstone intercalated with marl and evaporitic rocks, representing a near-shore setting (Fig. 6).

In the South Qiangtang depression, the coeval deposits are those of the Sewa and Quse Formations. The Quse Formation is distributed widely in the South Qiangtang depression, and has a thickness ranging from 680 to 1537 m (Zhao et al., 2000; Wang et al., 2009). The Quse Formation contains shale, siltstone, mudstone, and marl intercalated with fine sandstone (Fig. 4). Sedimentary structures such as horizontal bedding and convolute bedding were well developed, which is interpreted as shelf deposits (Fig. 6). The Sewa Formation strata conformably overly the Quse Formation strata in the South Qiangtang depression with a thickness ranging from 1023 to 1330 m (Wang et al., 2004a).

2.2.3. *The middle Jurassic Buqu Formation*

The Buqu Formation is of Middle Jurassic age (Bathonian) based on bivalve and brachiopod assemblages (Chengdu Institute of Geology and Mineral Resources, 2005a, b; Zhao et al., 2000). This unit covers the entire basin with a thickness ranging from 142 to 1446 m (Fig. 4). The Buqu Formation conformably overlies the

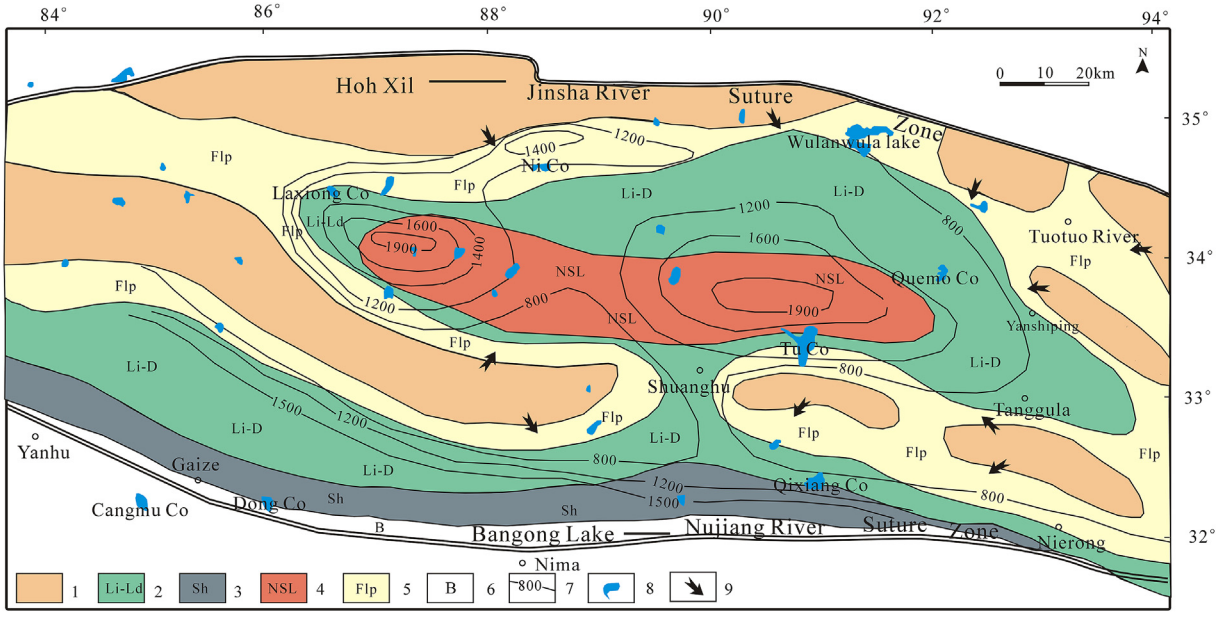

Fig. 6. Early-Middle Jurassic (Bajocian) paleogeographic and depositional environment maps of the Qiangtang Basin (modified from Wang et al., 2004a). 1, Erosion area; 2, Littoral–delta facies; 3, Shelf facies; 4, Near-shore lacustrine; 5, fluvial and alluvial facies; 6, Basin facies; 7, Thickness contour (m); 8, Lake; 9, Provenance.

Quemo Co Formation and the Sewa Formation in the basin. The sedimentary rocks of the Buqu Formation are made up of micritic limestone, marl, bioclastic limestone, oolitic limestone, oncolitic limestone, reef limestone, and dolomite intercalated with mudstone and shale (Fig. 4). Abundant bivalve, brachiopod, and encrinite were observed (Chengdu Institute of Geology and Mineral Resources, 2005a, b). Sparse ammonites has been observed in mudstone (Chengdu Institute of Geology and Mineral Resources, 2005b; Wang et al., 2009), together with high organic matter contents (Wang et al., 2004a) and well-preserved fossils (Chengdu Institute of Geology and Mineral Resources, 2005a, b), suggesting a carbonate platform (open and/or restricted platform) environment (Fig. 7).

2.2.4. The late Middle Jurassic Xiali Formation

During the late Middle Jurassic (Callovian), the Qiangtang Basin underwent a large-scale regression, resulting in deposition of mainly clastic sedimentary rocks interbedded with carbonates and gypsum of the Xiali Formation (Fig. 4). This unit conformably overlies the Buqu Formation, and has a thickness of 400–800 m (Fig. 4). The fine-grained sandstones and mudstones (about 800 m thickness) were well developed in the middle part of the basin, while coarse-grained sandstones (about 400 m thickness) occurred mainly in front of the surrounding mountainous areas (Fig. 8). Tidal flat-lagoon facies mudstone and shale were developed in the middle part of the basin, whereas rivers and deltas distributed along the margin of the basin (Fig. 8).

2.2.5. The upper Jurassic Suowa Formation

During Late Jurassic, the Suowa Formation formed an upward-fining transgression sequence consisting of coarse-grained limestones in the lower part, changing to marl and micritic limestone in the upper part (Fig. 4). The depo-center was located in the northwestern part of the North Qiangtang depression (Fig. 9), and the lithofacies are mainly composed of micritic limestone, marl, and shale. In the South Qiangtang depression, the Suowa Formation is made up of bioclastic limestone, oolitic limestone, oncolitic limestone, and reef limestone, suggesting an open platform environment (Fig. 9). The carbonates of the Suowa Formation in the Qiangtang Basin range from 283 to 1825 m in thickness (Fig. 4).

2.2.6. The late Jurassic to early Cretaceous Bailong Binghe Formation and Xueshan Formation

During Late Jurassic to Early Cretaceous, the Bangong ocean was closed by northward subduction beneath the Qiangtang terrane (Kapp et al., 2003), resulting in a large-scale regression in the Qiangtang Basin (Wang et al., 2004a). During this interval, the sediments only deposited in the North Qiangtang depression (Zhao et al., 2000) (Fig. 10) consisting of the Bailong Binghe and Xueshan Formations. The Bailong Binghe Formation is composed largely of marl, mudstone, calcarenite, and shale intercalated with oil shale and evaporitic rocks (Fig. 4), and has the maximum thickness of approximately 2080 m. The Bailong Binghe Formation is characterized by abundant bivalve and ammonite fossils, with subordinate occurrence of worm trails. Sedimentary structures such as horizontal bedding and convolute bedding are well developed and indicate a shelf to restricted-platform facies environment (Fig. 10).

The Xueshan Formation is composed of sandstone, mudstone, and minor conglomerate with a thickness ranging from 532 to 1430 m (Chengdu Institute of Geology and Mineral Resources, 2005a, b). This unit is distributed mainly along the margin of the North Qiangtang depression (Fig. 10). The lower part of the unit is composed largely of mudstone and quartz sandstone intercalated with salt, and contains brackish and fresh water fossils, suggesting a deltaic environment (Fig. 10). The upper part of the unit is typically conglomeratic with characteristics of fluvial deposition (Fig. 4). The overall facies of the Xueshan Formation indicates a shallowing-upward trend (Wang et al., 2004a). During Late Cretaceous, marine deposition ended and a period of terrestrial deposition began in the Qiangtang Basin.

3. Samples and analytical methods

3.1. Sampling and analytical methods for source rocks

Sections were measured to evaluate the thickness of source

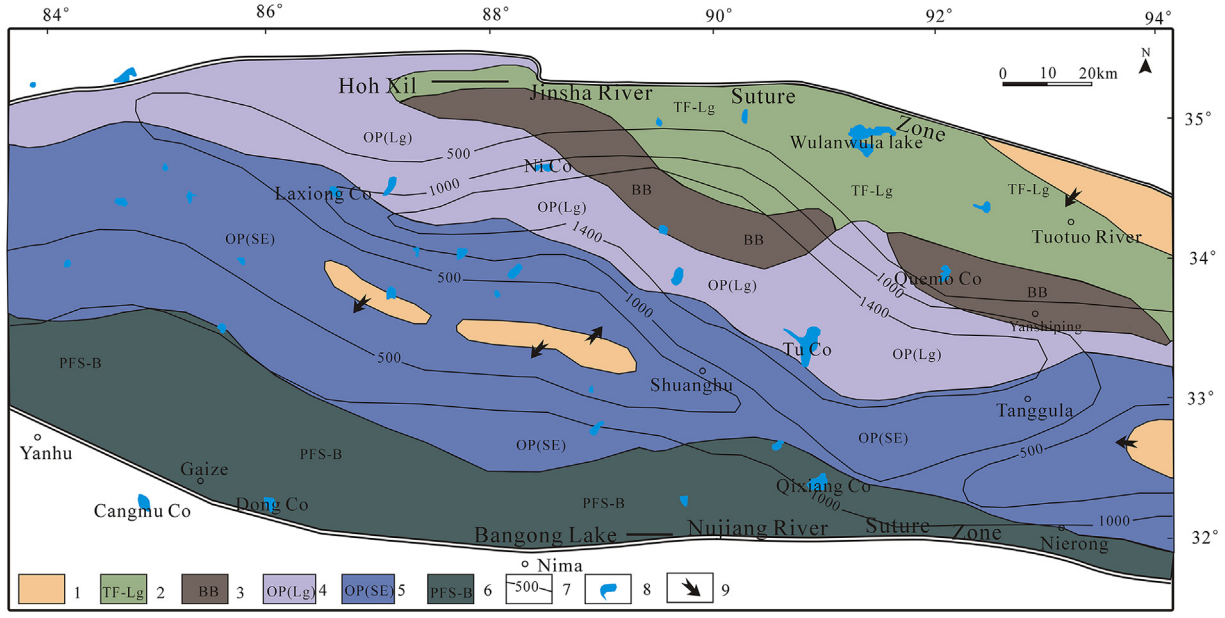

Fig. 7. Bathonian (Middle Jurassic) paleogeographic and depositional environment maps of the Qiangtang Basin (modified from Wang et al., 2004a). 1, Erosion area; 2, Tidal –lagoon facies; 3, Barrier beach; 4, Open platform (including lagoon) facies; 5, Open platform (including shoal on edge of platform) facies; 6, Foreslope of platform-basin facies; 7, Thickness contour (m); 8, Lake; 9, Provenance.

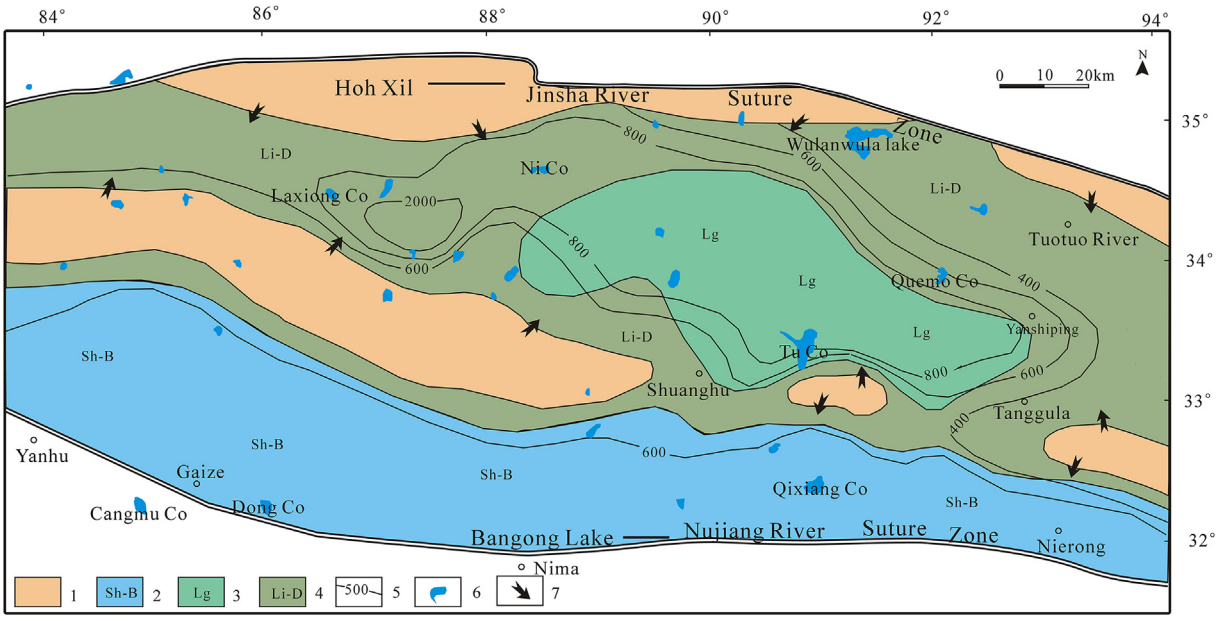

Fig. 8. Callovian (Middle Jurassic) paleogeographic and depositional environment maps of the Qiangtang Basin (modified from Wang et al., 2004a). 1, Erosion area; 2, Shelf –basin facies; 3, Lagoon facies; 4, Littoral –delta facies; 5, Thickness contour (m); 6, Lake; 7, Provenance.

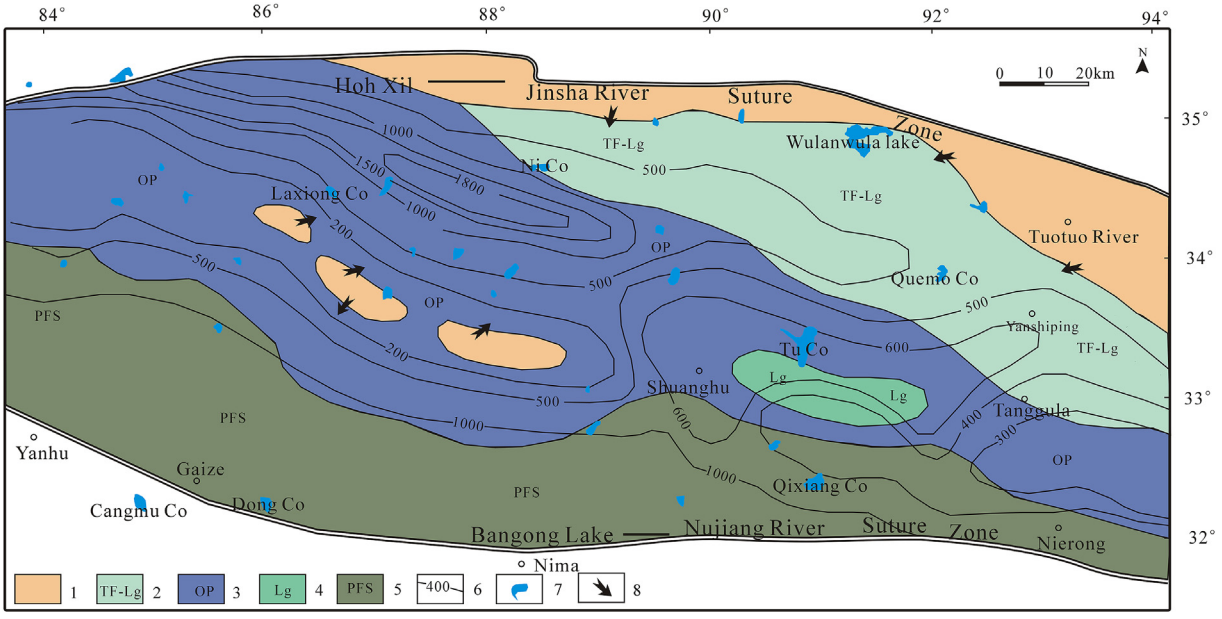

Fig. 9. Late Jurassic paleogeographic and depositional environment maps of the Qiangtang Basin (modified from Wang et al., 2004a). 1, Erosion area; 2, Tidal –lagoon facies; 3, Open platform facies; 4, Lagoon facies; 5, Foreslope of platform; 6, Thickness contour (m); 7, Lake; 8, Provenance.

rocks. The detailed section locations are presented in Figs. 11a, 12a and 13a, and 14a. 1113 source rocks were picked up from nine Formations, including Suowa Formation, Xiali Formation, Buqu Formation, Quemo Co Formation, Sewa Formation, Quse Formation, Tumen Gela Formation, Rejue Chaka Formation, and Chameng Formation (Table 1).

Total organic carbon (TOC) measurements used a LECO-analyzer on acidified samples. Analytical procedures are referenced from Yeomans and Bremmer (1989). The pulverized samples were extracted with chloroform in a Soxhlet apparatus for 72 h (Yang et al., 1997). Kerogen isolation was performed on about 50 g of sample (ground to less than 200 meshes). These samples were treated with HCl/HF following the method of Bishop et al. (1998). After treatment with HCl/HF, the leached samples were cleaned using de-ionized water until they were neutral, and subsequently extracted with benzene/acetone (2:5 v/v) for 72 h in order to remove the dissolved organic matter (Chen et al., 2005). Finally, the extracted kerogens were rinsed using de-ionized water, then frozen and freeze-dried for separation. Vitrinite reflectance (Ro) measurements were performed using a Leica MPV Compact II reflected light microscope fitted with an oil-immersion photomicrometer (Zeng et al., 2013).

The source rock samples from outcrops and three shallow wells (QZ-1, QZ-2, and QZ-4, Fig. 1) in the North Qiangtang depression are

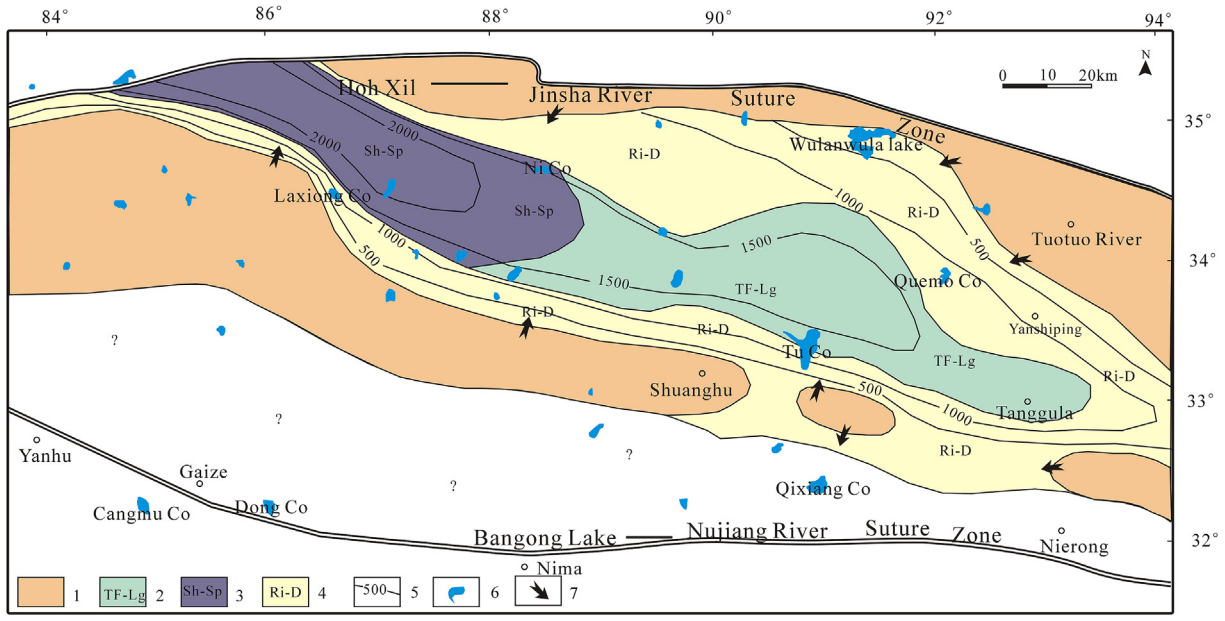

Fig. 10. Late Jurassic to early Cretaceous paleogeographic and depositional environment maps of the Qiangtang Basin(modified from Wang et al., 2004a). 1, Erosion area; 2, Tidal–lagoon facies; 3, Shelf to restricted-platform facies; 4, River-delta facies; 5, Thickness contour (m); 6, Lake; 7, Provenance.

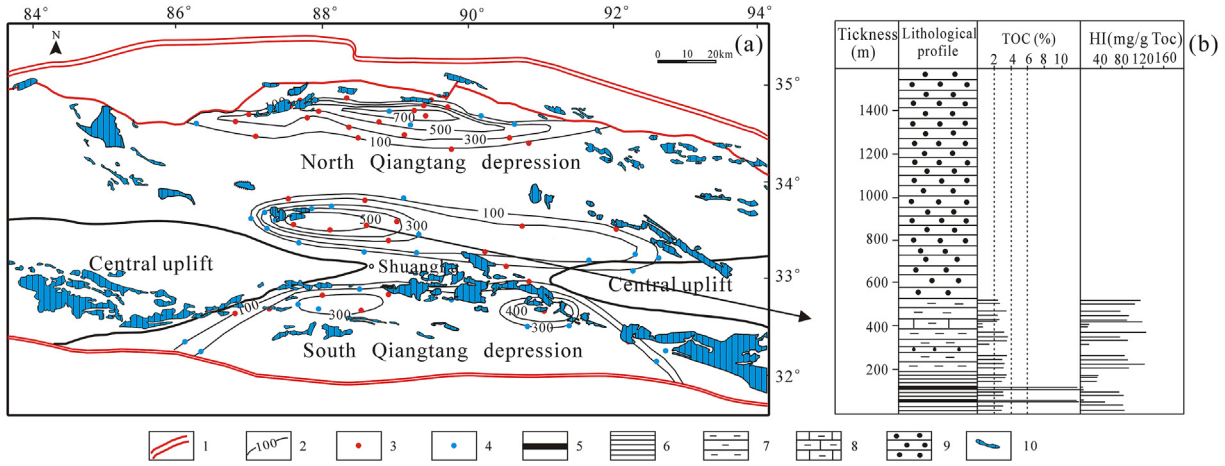

Fig. 11. (a) Map showing the extent of Upper Triassic potential source rocks in the Qiangtang Basin (unit: m) (modified from Fu et al., 2013) and (b) lithostratigraphic column for the Tumen Gela Formation and the variation in TOC and HI values in the section. 1, Suture; 2, Thickness contour (m); 3, Measured section of this study; 4, Measured section from the literature (Zhao et al., 2000; Wang et al., 2004a; Wang et al., 2009; Ding et al., 2011); 5, coal; 6, shale; 7, mudstone; 8, Marl; 9, sandstone; 10, Upper Triassic outcrop.

used to model the thermal maturity of the source rocks. The geothermal gradient (T) is given by T=(T1-T2)/H, where T1 and T2 are the analytical temperatures of inclusions in location 1 and location 2, respectively, and H is the "vertical" distance between location 1 and location 2. The geothermal gradient in the middle part of the North Qiangtang depression is around 2.64 °C/100 m (Fu et al., 2013), and the surface heat flow is approximately 46.69 mW/m^2 (He et al., 2014).

3.2. Sampling and analytical methods for reservoirs and seals

Sections were measured to evaluate the thickness of reservoir rocks and seals. Three hundred and seventeen samples were collected to evaluate the physical characteristics of reservoir rocks. Ninety limestone samples were collected from the Suowa Formation; eighty-four sandstone samples were collected from the Xiala Formation; forty-one dolomite samples were collected from the Buqu Formation; and one hundred and two sandstone samples were collected from the Quemo Co Formation (Table 2).

The mineralogy was determined by optical microscopic observation and powder X-ray diffraction (XRD). The XRD measurements were carried out at Tianjin Center, China Geological Survey using a D8 ADVANCE diffractometer equipped with a Cu-target tube and a curved graphite monochromator. The XRD pattern was recorded over a 2θ interval of 5–70°, with a step size of 0.02°. Porosity and permeability were determined in the Chengdu University of Technology following the method described by Delbrouck et al. (1993).

3.3. Evaluated methods for favorable areas

The favorable areas were evaluated by studying the sedimentary facies, source rocks, reservoir rocks, cap rocks, traps, and

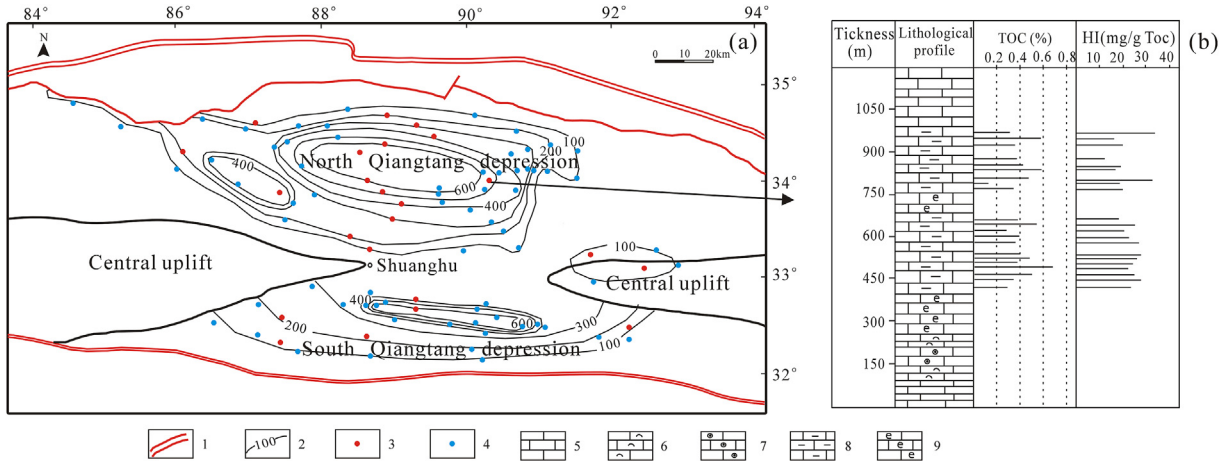

Fig. 12. (a) Distribution of hydrocarbon source rocks of the Buqu Formation in the Qiangtang Basin (unit: m) and (b) lithostratigraphic column for the Buqu Formation and the variation in TOC and HI values in the section. 1, Suture; 2, Thickness contour (m); 3, Measured section of this study; 4, Measured section from the literature (Zhao et al., 2000; Wang et al., 2004a; Wang et al., 2009; Ding et al., 2011); 5, micritic limestone; 6, shell limestone; 7, oolitic limestone; 8, Marl; 9, bioclastic limestone.

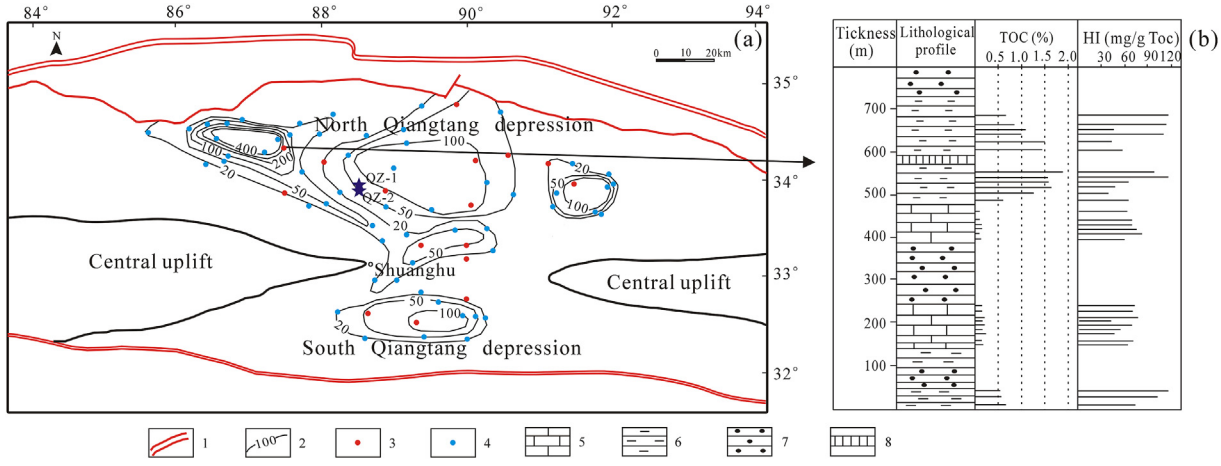

Fig. 13. (a) Distribution of hydrocarbon source rocks of the Xiali Formation in the Qiangtang Basin (unit: m) and (b) lithostratigraphic column for the Xiali Formation and the variation in TOC and HI values in the Section. 1, Suture; 2, Thickness contour (m); 3, Measured section of this study; 4, Measured section from the literature (Zhao et al., 2000; Wang et al., 2004a; Wang et al., 2009; Ding et al., 2011); 5, micritic limestone; 6, mudstone; 7, sandstone; 8, gypsum and salt.

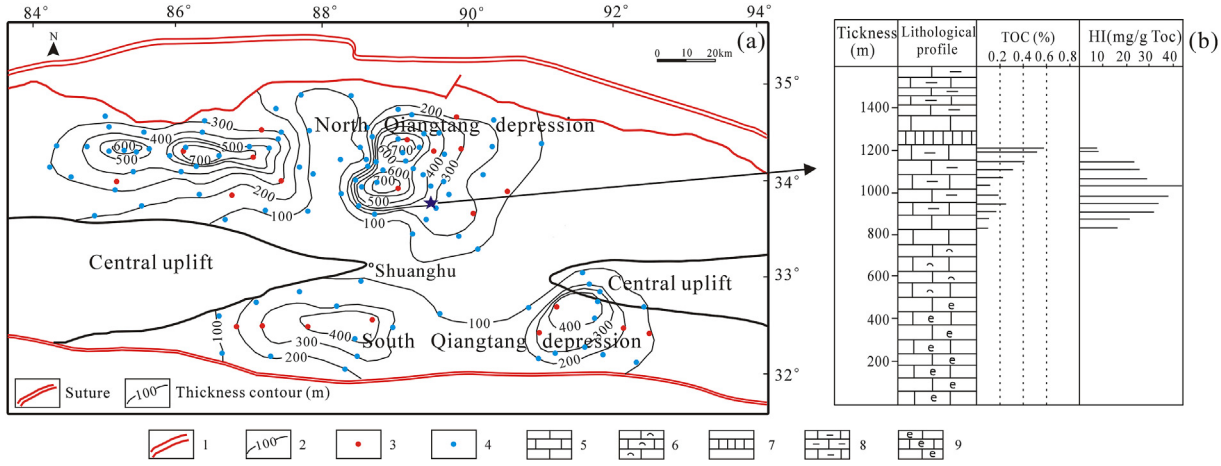

Fig. 14. (a) Distribution of hydrocarbon source rocks of the Suowa Formation in the Qiangtang Basin (unit: m) and (b) lithostratigraphic column for the Suowa Formation and the variation in TOC and HI values in the Section. 1, Suture; 2, Thickness contour (m); 3, Measured section of this study; 4, Measured section from the literature (Zhao et al., 2000; Wang et al., 2004a; Wang et al., 2009; Ding et al., 2011); 5, micritic limestone; 6, shell limestone; 7, gypsum and salt; 8, Marl; 9, bioclastic limestone.

Table 1
Thickness and geochemical features of main source rocks in the Qiangtang Basin.

Stratigraphic unit		Lithology	Average Thickness, m	TOC (%)				Average "bitumen" A (ppm)	HI (mg/g Toc)	Kerogen type	Ro (%)
				Max.	Min.	Avg.	n				
Carboniferous	Chameng Formation	Shale	35 (115)	1.97	0.20	1.10	22	1800	0.3–7.1	III	2.06–2.37
Permian	Rejue Chaka Formation	Mudstone	81 (266)	2.49	0.61	1.27	26	140	12.2–95.1	III	1.27–3.73
Triassic	Tumen Gela Formation	Mudstone	420 (1378)	3.45	1.25	2.20	108	930	2.8–123	II	0.94–3.00
Jurassic	Quse Formation	Mudstone	172 (564)	26.1	0.40	0.51	119	608	47–580	II	1.58–2.38
	Sewa Formation	Mudstone	120 (394)	1.07	0.58	0.83	30	111	5.2–36.5	II	1.32–2.21
	Quemo Co Formation	Mudstone	22 (72)	0.80	0.47	0.56	24	120	7.8–39.5	II	1.46–2.19
	Buqu Formation	Carbonate	230 (755)	0.68	0.12	0.21	392	230	7.0–223	II	1.30–2.38
	Xiali Formation	Mudstone	167 (548)	7.30	0.55	1.05	120	250	7.0–165	II	1.06–1.42
		Carbonate	85 (279)	1.63	0.10	0.13	44	261	10–66	II	
	Suowa Formation	Carbonate	200 (656)	1.91	0.10	0.21	228	66.5	5.0–157	II or I	0.74–1.30

TOC = total organic carbon. Max. = maximum TOC values. Min. = minimum TOC values. Avg. = average TOC values. n = number of samples.

Table 2
Thickness and physical parameter of main reservoir rocks in the Qiangtang Basin.

Stratigraphic unit		Lithology	Average thickness, m (ft)	Porosity (%)				Permeability (mD)			
				Max.	Min.	Avg.	n	Max.	Min.	Avg.	n
Jurassic	Quemo Co Formation	Sandstone	520 (1706)	9.27	1.30	3.54	102	6.45	0.05	1.35	102
	Buqu Formation	Dolomite	100 (328)	15.5	2.37	9.77	41	14.6	0.58	5.25	41
	Xiala Formation	Sandstone	200 (656)	8.30	1.94	3.19	84	54.8	0.06	5.81	84
	Suowa Formation	Limestone	280 (919)	16.9	0.13	2.90	90	47.5	0.12	5.17	90

Max. = maximum values. Min. = minimum values. Avg. = average values. n = number of samples.

preservation of oil and gas resources. The evaluation method is given below.

The first step was to recognize good source-reservoir-caprock assemblages. Then we evaluated source rocks, reservoir rocks, and top seals individually, and identified favorable source-rock, reservoir-rock and cap-rock areas for each good source-reservoir-caprock assemblage. The favorable source-rock areas were predicted on the basis of fully considering the petrologic characteristics, thickness, TOC content, kerogen type, thermal evolution, and hydrocarbon generation potential of source rocks and sedimentary facies. The favorable reservoir-rock areas were predicted on the basis of petrologic characteristics, thickness, porosity, and permeability of reservoir rocks, and fully considering the distribution of paleo-karst and sedimentary facies. The favorable top seals areas were predicted on the basis of petrologic characteristics, thickness, porosity, and permeability of cap rocks, and fully considering the distribution of evaporitic beds and sedimentary facies. The third step was to analyze tectonic activity, and to predict favorable areas for preservation of oil and gas resources. The factors considered in this step included tectonic movement intensity, episodes of tectonic activity, tectonic uplift and erosion, fracture features, degree of metamorphism in rocks, magmatism, and groundwater were also considered in this step. The fourth step was to evaluate favorable traps, which are based on fully considering structural trap size, timing of trap formation, fault development, and peak oil and gas generation. Based on these data, as well as combined with basin tectonic framework and evolution, we proposed six favorable belts. Finally, the favorable belts were studied by three surveys: a geological survey for oil and gas (1: 50, 000), a geochemical survey, and a seismic survey. The seismic grid reached 4 × 4 to 8 × 8 km^2 (1.54 × 1.54–3.09 × 3.09 mi^2) in the main region. The geochemical survey is based on soil sample analyses. Soil samples were collected at the depth of 60 cm, and each sample weighed approximately 1 kg, following the method described by Sun et al. (2014).

4. Results and discussion

4.1. Hydrocarbon geological characteristics

4.1.1. Source rocks

The thickness and geochemical features of the main source rocks in the Qiangtang Basin are presented in Table 1 and Supplementary Tables 1, 2, and 3. Table 1 also contains potential source rocks from Paleozoic strata. The important source rocks (Fig. 4) in the basin include the Triassic Tumen Gela Formation mudstone, Jurassic Buqu Formation carbonate, Xiali Formation, and Suowa Formation mudstone and carbonate.

Plan-view distribution of Tumen Gela Formation source rocks in the Qiangtang Basin is shown in Fig. 11a and their changes across the basin are shown in Fig. 15, which are composed of 42.0–645.8 m of black mudstones (or shales), 29.0–404.0 m of carbonates, and 0–10 m of coals (Fig. 11b) with high TOC contents, representing the main source rock in the basin. Coal-bearing strata generally exhibit higher TOC content, as compared with mudstone and marl samples (Fig. 11b). The TOC content of black mudstones developing within the Tumen Gela Formation ranges from 1.25 to 3.45%, and HI values range 2.8–123 mg/g Toc (Table 1 and Supplementary Table 2). The average content of extracted bitumen is about 930 ppm (Table 1). Petrographically, the Tumen Gela mudstones are characterized by a vitrinite content of 10–19%, an inertinite content of 27–42%, and slightly high saprovitrinite content of 51–68%. All these observations indicate that the kerogen type in Tumen Gela mudstones is mainly type II (Table 1). The source rocks of the Tumen Gela Formation reached peak oil generation in the Early Callovian (about 164 Ma), entered the wet-gas window at the middle of the Late Jurassic (about 157 Ma), and reached dry-gas window at about 148 Ma (Fig. 16). Most of the Tumen Gela Formation is within both wet-gas and dry-gas windows, with a corresponding Ro in the range of 0.94–3.00% (Table 1).

Distribution of Buqu Formation source rocks in the Qiangtang Basin is shown in Fig. 12a and their changes across the basin are

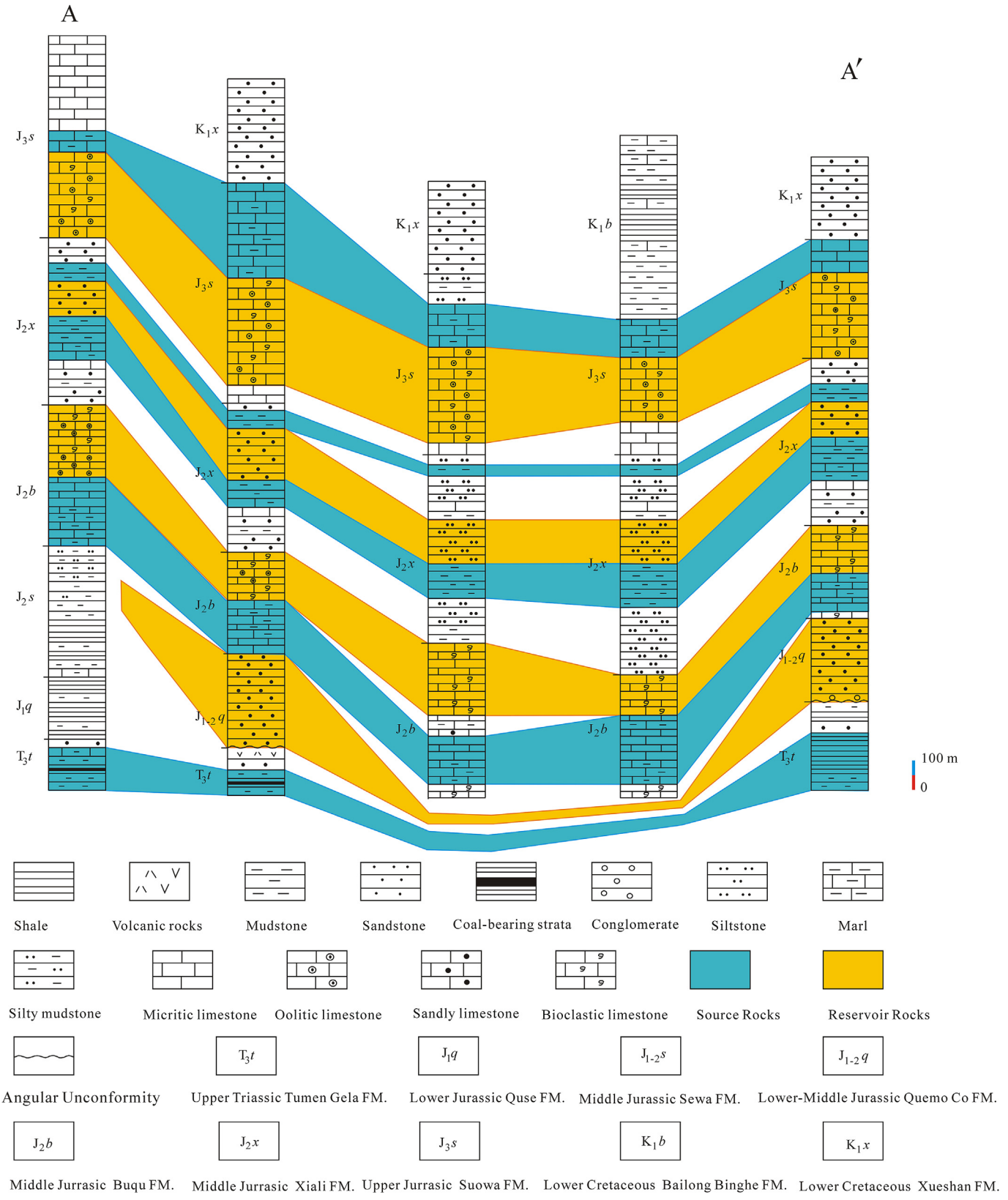

Fig. 15. South-north cross section AA', showing source rock and reservoir rock changes across the basin. The line of the section is shown in Fig. 1b.

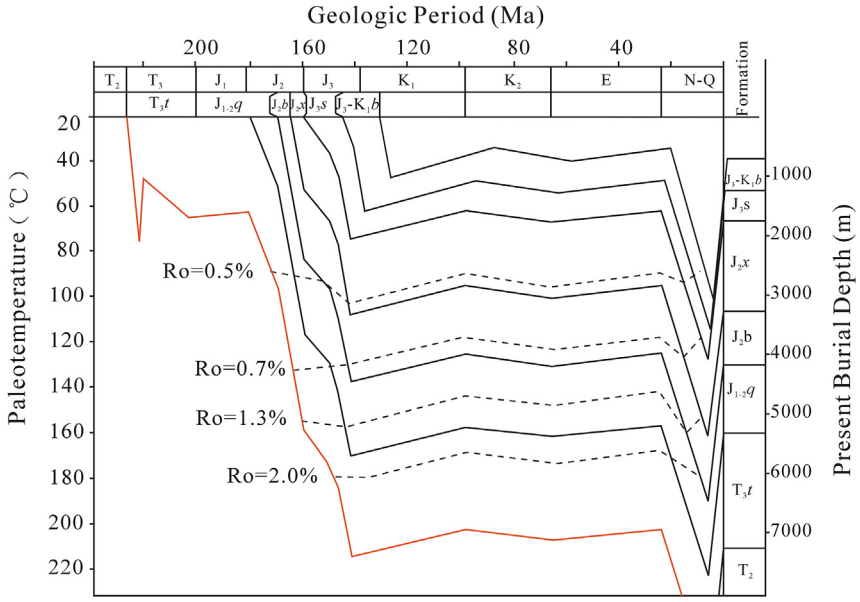

Fig. 16. Basin-modeling result showing the possible thermal evolution of the source rocks with geologic era in the middle part of the North Qiangtang depression. T_3t = Tumen Gela Formation; $J_{1-2}q$ = Quemo Co Formation; J_2b = Buqu Formation; J_2x = Xiali Formation; J_3–K_1b = Bilong Binghe Formation.

shown in Fig. 15. The Middle Jurassic carbonates of the Buqu Formation have a low-to-middle content of organic matter (Fig. 12b, Table 1, Supplementary Table 3), showing poor-to-fair quality. The Longeni paleo-oil-reservoir zone recognized in the South Qiangtang depression was partly from the Buqu source rocks, which is proved by oil-source rock correlation (Fu et al., 2008). The carbonates of the Buqu Formation in the Qiangtang Basin have a thickness ranging from 67.0 to 631.3 m. The TOC content of the Buqu carbonates ranges from 0.12 to 0.68%, averaging 0.21% (Table 1). The average content of chloroform-extract bitumen is about 230 ppm (Table 1). The HI values range from 7.0 to 223 mg/g Toc (Supplementary Table 3). Under the microscope, the saprovitrinite content of the Buqu carbonates ranges from 62 to 88%, and the inertinite content ranges from 9 to 33%. The Buqu Formation is characterized by a low vitrinite content ranging from 3 to 8%. These observations indicate that the kerogen in Buqu carbonates is mainly type II. The source rocks of the Buqu Formation reached peak oil generation during the Early Cretaceous (about 143 Ma), entered the wet-gas window during the Neogene (about 15 Ma), and reached the dry-gas window at about 7 Ma (Fig. 16). Most of the Buqu Formation is within the oil and wet-gas windows, with a corresponding Ro in the range of 1.30–2.38% (Table 1).

Distribution of Xiali Formation source rocks in the Qiangtang Basin is shown in Fig. 13a and their changes across the basin are shown in Fig. 15. The Middle Jurassic Xiali Formation has an average thickness of 167 and 85 m for mudstones and carbonates, respectively. The mudstone samples generally exhibit higher total organic carbon content compared to carbonate samples (Fig. 13b). The average TOC content in Xiali mudstones is about 1.05%, while the Xiali carbonates exhibit a lower TOC content ranging from 0.10 to 1.63%, with an average of 0.13% (Table 1). The high TOC source rocks for the Xiali carbonates are distributed locally in the central part of the North Qiangtang depression. The average content of chloroform-extract bitumen is about 250 and 161 ppm for the Xiali mudstones and carbonates, respectively (Table 1). The HI values range from 7.0 to 165 and 10–66 for the Xiali mudstones and carbonates, respectively (Supplementary Table 3). Under the microscope, the Xiali carbonates exhibit slightly high saprovitrinite content (70–87%), and low inertinite (10–25%) and vitrinite (3–9%) contents, indicating that the kerogen in Xiali carbonates is mainly type II. The Xiali mudstones exhibit slightly high saprovitrinite (38–60%) and inertinite contents (19–30%), and low vitrinite content (20–27%), indicating that the kerogen type in Xiali mudstones is mainly type II, and partly type III. The source rocks of the Xiali Formation entered the oil window during the Early Cretaceous (about 145 Ma), and reached peak oil generation at about 17 Ma (Fig. 16). Because of uplift and erosion of the basin, the activity of hydrocarbon generation gradually declined. At the present time, the Xiali Formation source rocks straddle the border between oil and gas window with an associated Ro range of 1.06–1.42% (Table 1).

Distribution of Suowa Formation source rocks in the Qiangtang Basin is shown in Fig. 14a and their changes across the basin are shown in Fig. 15. The shallow-well data indicate that the high TOC content source rocks are located mainly in the middle part of the Suowa Formation strata (Fig. 14b). The Upper Jurassic carbonates of the Suowa Formation have a low content of organic matter, showing poor to fair quality as hydrocarbon source rocks. The Suowa carbonates in the Qiangtang Basin range from 40.0 to 760.0 m in thickness. The average and maximum TOC contents in the Suowa carbonates are 0.21 and 1.91%, respectively (Table 1). The high TOC source rocks for the Suowa carbonates are locally distributed in the central and western parts of the North Qiangtang depression. The average content of chloroform-extract bitumen is about 66.5 ppm (Table 1). The HI values range from 5.0 to 157 mg/g Toc (Supplementary Table 3). The saprovitrinite content in Suowa carbonates ranges from 65 to 95%, with the vitrinite content ranging from 2 to 8% and the inertinite content from 4 to 29%. These observations indicate that the kerogen in Suowa carbonates is mainly type II, and partly typeI. The source rocks of the Suowa Formation entered the oil window during the Neogene (about 13 Ma), and reached peak oil generation at about 6 Ma (Fig. 16). At the present time, most of the Suowa Formation is within the oil window, with a corresponding Ro range of 0.74–1.30% (Table 1).

4.1.2. Reservoir rocks

Several potential reservoirs, as discussed below, occur in the Qiangtang Basin, including Buqu Formation dolomite, pre-Nadi

Kangri paleo-weathered crust, Quemo Co Formation and Xiali Formation sandstones, and Suowa Formation limestone.

Most of the oil discovered in the Qiangtang Basin is located in the Buqu Formation. The reservoir rocks are predominantly dolomites, which are distributed mainly in the southern Qiangtang depression. In 2000, a large paleo-oil-reservoir zone was discovered in the South Qiangtang depression (Wang et al., 2004b). This zone is exposed for a distance of more than 100 km in the east-west direction. The thickness of dolomite in the Buqu Formation is 2–400 m thick. On the basis of evidence from well-log data (QZ-3 in Fig. 1) (Fig. 17a), we infer that the dolomite deposited in tidal flat environments. Strong compaction due to deep burial has led to marked reduction in primary porosity, whereas secondary porosity formed by burial dolomitization has contributed significantly to the present-day porosity (Fig. 17c). Forty-one dolomite samples were collected from two shallow wells (QK-1 and QZ-3 in Fig. 1) for porosity and permeability analyses. The measured core porosity ranges from 2.37 to 15.5% (9.77% average), while permeability varies between 0.58 and 14.6 mD (5.25 mD average) (Table 2, Fig. 18a). Although tight, the Buqu Formation dolomites are highly oil-bearing. Our statistical results show that dolomite samples of the Buqu Formation from two shallow wells have average oil and bitumen concentrations of 5.0% and 6.2%, respectively. Therefore, the Buqu Formation dolomites are the most likely reservoir in the basin.

The pre-Nadi Kangri paleo-weathered crusts are also potential reservoirs in the Qiangtang Basin, because the dissolution pores and holes are very well developed. The paleo-weathered crusts occur at the top of the Permian strata in the central uplift and the South Qiangtang depression, and at the top of the Tumen Gela strata in the North Qiangtang depression, respectively (Fu et al., 2009). They are overlain unconformably by the Nadi Kangri volcanic rocks with a thickness of a few tens of centimeters (Fu et al., 2010a). Regionally, the paleo-weathered crusts were well developed in the North Qiangtang depression, the central uplift and the South Qiangtang depression (Fu et al., 2009). In the outcrops, they can be further divided into three broad units based on sedimentary features including paleokarst zone, dissolution breccia and weathered claystone layers (Fu et al., 2010a). The lower paleokarst zone with a thickness of 35–60 cm shows a gradational transition from unweathered rocks to weathered sequences. Above the paleokarst zone, a succession of dissolution breccias with a thickness of 30–70 cm occurs. The dissolution breccia zone is overlain by a succession of weathered claystones. These claystones are mainly composed of brown and red mottled clays, sandy in some places, with a thickness of 3–10 cm (Fu et al., 2010a). Dissolved pores, caves, and fractures are the main porosity types.

The Quemo Co Formation alluvial and fluvial sandstones and the Xiali Formation littoral sandstones also represent important reservoirs in the Qiangtang Basin. The Quemo Co sandstones are distributed locally along the margin of the basin and the central uplift, with the thicknesses of 300–1000 m. Measured porosity from 102 outcrop samples (fluvial sandstones) ranges from 1.30 to 9.27% (3.50% average), while permeability varies between 0.05 and 6.45 mD (1.35 mD average) (Table 2, Fig. 18b). The Xiali sandstones are distributed locally in the central and western parts of the basin with an average thickness of 200 m. Measured porosity values from 2 shallow wells (QZ-1 and QZ-2, Fig. 1) range from 0.84 to 8.30% (3.47% average), while permeability varies between 0.06 and 54.8 mD (5.81 mD average) (Table 2, Fig. 18c).

Additionally, limestones in the Suowa Formations can also form oil and/or gas reservoirs. They consist of reef limestone, oolitic limestone, and bioclastic limestone. According to outcrop and drilling data (QZ-4), the Souwa limestones are usually 100–300 m in thickness with a maximum of 627.9 m. Laterally, the Suowa Formation limestones are the thickest in the central part of the North Qiangtang depression (Wang et al., 2004a). The Suowa limestones have average porosity and permeability of around 2.90% and 5.17 mD, respectively (Table 2, Fig. 18d).

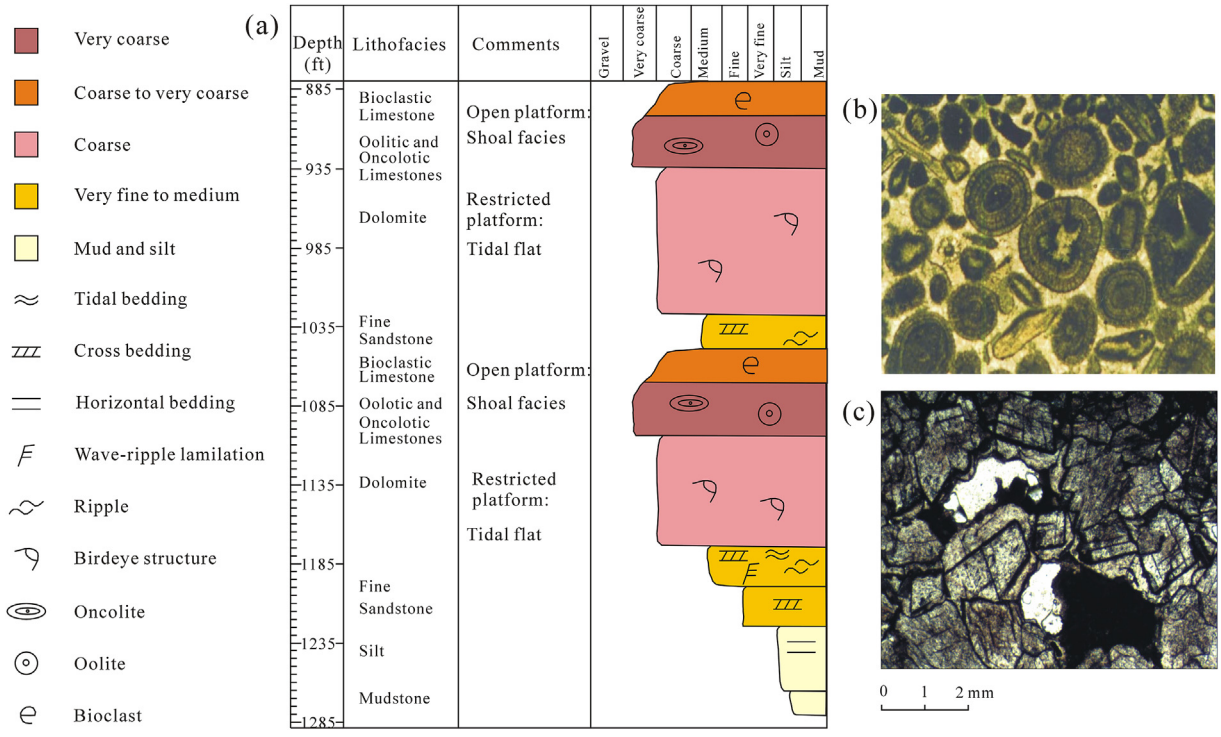

Fig. 17. (a) Core description of QZ-3 well, and photographs of oolitic limestone (b) and dissolved porosity of dolomite (c).

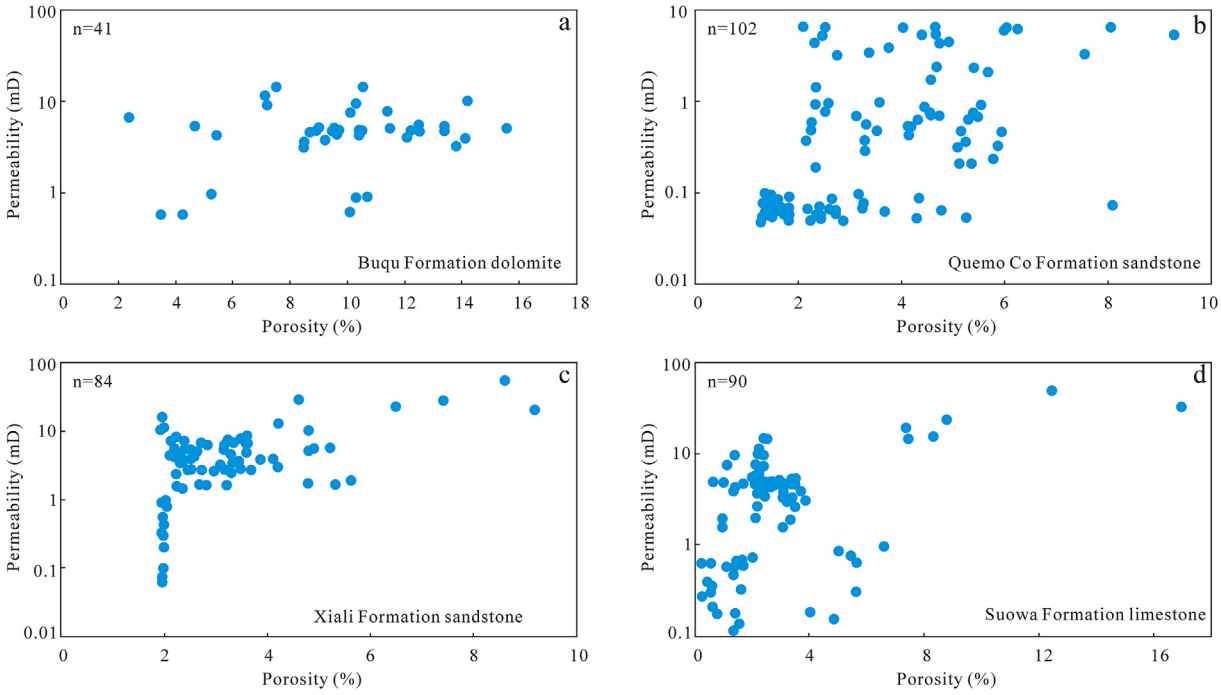

Fig. 18. Relationships between porosity and permeability of the reservoirs in the Qiangtang Basin.

4.1.3. Seals

Three regional seals are identified in the Qiangtang Basin, including Quse Formation mudstones (or shales), Bailong Binghe Formation marls, and Buqu Formation micritic limestones.

The Quse Formation mudstones (or shales) and the Bailong Binghe Formation marls represent the most important regional seals in the Qiangtang Basin. The Quse mudstone is widespread in the South Qiangtang depression with individual bed thickness ranging from 94 to 133.8 m. According to x-ray diffraction data from outcrop samples, the clay minerals in the mudstones are mainly kaolinite and illite. The average breakthrough pressure of the Sewa mudstone is about 11.7 Mpa (Wang et al., 2009). The Quse mudstones are thus a good regional seal in the South Qiangtang depression.

Bailong Binghe Formation strata were widely developed in the North Qiangtang depression, containing evaporitic rocks, shale (or oil shale), and marl. From the measured sections in the North Qiangtang depression and a shallow well data (QZ-4, Fig. 1), the total shale thickness is 0.5–13.0 m in the central part of the North Qiangtang depression, which includes 4 to 7 shale (or oil shale) beds. The total thickness of the evaporitic rocks is about 31.0–188.4 m, and the total thickness of the marl is 358.0–560.0 m. The marl thickness decreases generally from the west to east, exceeding 560.0 m in the western part of the North Qiangtang depression. According to x-ray diffraction data from core samples (QZ-4 well, Fig. 1), the Bailong Binghe marl has an anhydrite content of 3–12%, and the average breakthrough pressure of the Bailong Binghe marl is about 6.38 Mpa (Wang et al., 2009). The Bailong Binghe marl thus serves as a good regional seal in the North Qiangtang depression.

The Buqu Formation micritic limestone can also serve as a regional seal in the Qiangtang Basin because of its widespread distribution; large individual bed thicknesses that are generally in the range of 45.7–127.8 m; lateral continuation; and high breakthrough pressure (7.21 Mpa average, Wang et al., 2009). From the measured sections, the total micritic limestone thickness is more than 200 m in the middle part of the South Qiangtang depression, which includes 3 to 6 gypsum beds that are each 0.3–16.0 m thick. The presence of evaporitic rocks further strengthens the seal capacity of the Buqu micritic limestone.

4.1.4. Potential traps

The traps in the Qiangtang Basin are mainly structural traps. Seventy-one potential anticlines are identified in the Qiangtang Basin, each of which occupies an area of more than 30 km^2 (Fu et al., 2013). Fifteen of them cover an area of more than 100 km^2 (Fu et al., 2013). These structural traps formed mainly during the Late Jurassic to Early Cretaceous, due largely to the closure of the Meso-Tethyan Ocean (Yin and Harrison, 2000). The traps formed before or during petroleum migration (Wang et al., 2009). Seismic data indicate that some traps are connected with the oil source by faults (Fu et al., 2013), forming a very favorable environment for hydrocarbon accumulation. In addition, lithological traps may develop in the South Qiangtang depression (Wang et al., 2004b).

4.2. Analyses on favorable hydrocarbon exploration areas

Nine favorable hydrocarbon exploration areas were identified in the Qiangtang Basin, of which the Tuonamu and Badaohu areas are selected as the key targets for exploration for oil and gas resources in the Qiangtang Basin, northern Tibet, China in the near future.

4.2.1. Tuonamu area

The Tuonamu area (about 2500 km^2 in total area) is located in the southern part of the North Qiangtang depression, where the Lower Cretaceous marine deposits were widely developed, including the Bailong Binghe Formation and the Xueshan Formation (Fig. 19). The Bailong Binghe evaporitic rocks, shale, and marl are widely distributed in the region and are good regional seals. The reservoirs consist of the Quemo Co Formation sandstone, the Buqu Formation oolitic limestones and the bioclastic limestones, Tumen Gela Formation coal-bearing mudstones and Buqu Formation

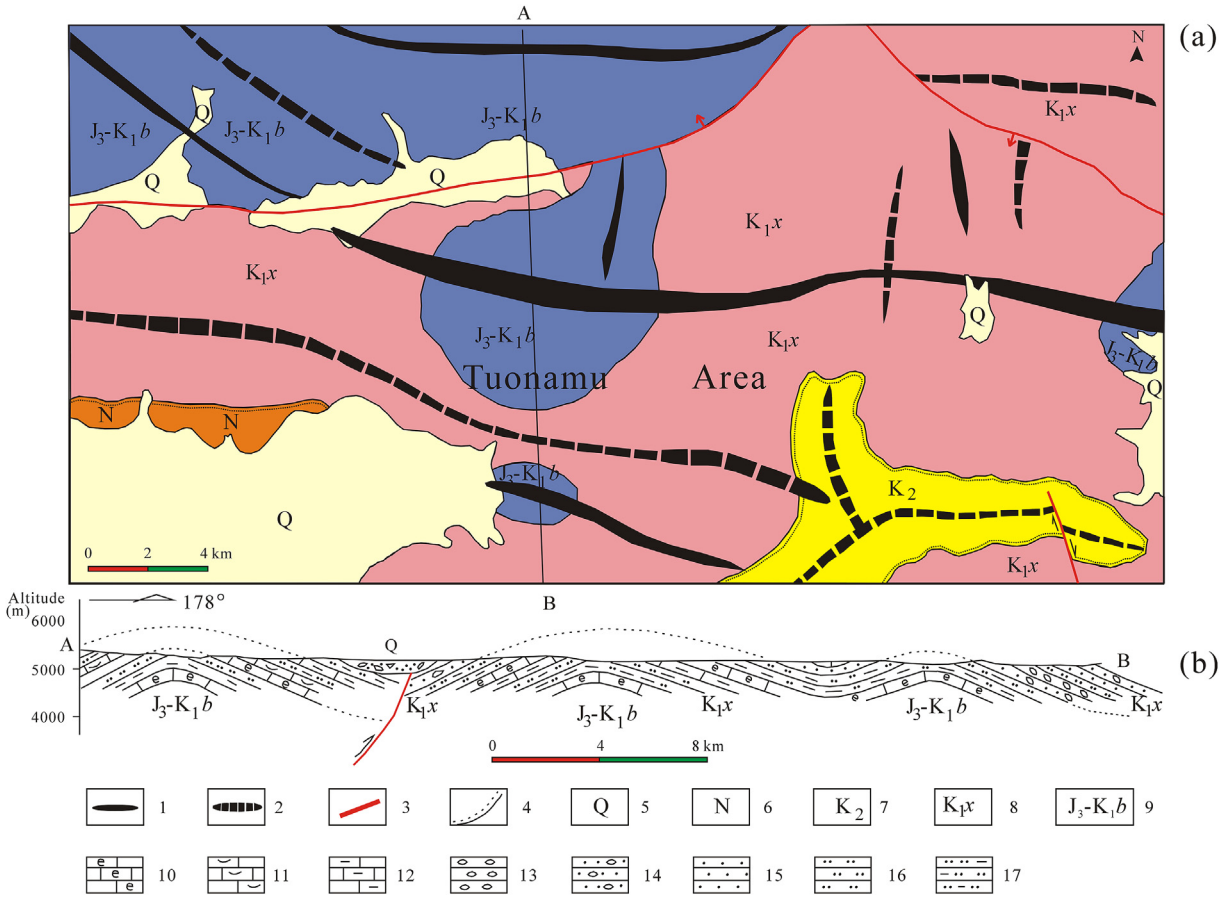

Fig. 19. Simplified tectonic map of the Tuonamu area in the Qiangtang Basin and schematic cross section (the location is in Fig. 16a) across this area (modified from Wang et al., 2009). 1, Anticline; 2, Syncline; 3, Fault; 4, Unconformity; 5, Quaternary; 6, Neogene; 7, Upper Cretaceous; 8, Xueshan Formation; 9, Bailong Binghe Formation; 10, bioclastic limestone; 11, coquina; 12, marl; 13; conglomerate; 14, sandy conglomerate; 15, sandstone; 16, siltstone; 17, muddy siltstone.

carbonates represent the major source rocks.

Four large-scale anticlines are identified by geological survey and seismic interpretation in the Tuonamu area (Fig. 19). These paleo-anticlines formed mainly during the Late Jurassic to Early Cretaceous (Wang et al., 2009), while the Buqu source rocks reached peak oil generation at ~143 Ma as discussed above. These paleo-anticline traps formed before peak petroleum generation.

The fault activation is relatively weak in the Tunomu area (Fig. 19a). However, two large faults have been found, and some oil and gas shows have also been found in the faults by field survey. The faults connect the paleo-anticlines to the source rocks (Fu et al., 2013), and the paleo-anticlines are near the hydrocarbon generation center. Therefore, large-scale paleo-anticlines are the most favorable targets in the Tuonamu area.

In addition to the conditions discussed above, we selected the Tuonamu area as one of the most favorable targets for oil and gas accumulation on the basis of the following four reasons:

(1) There are excellent preservation conditions in the Tuonamu area. The tectonic movements were very weak in the Tuonamu area after hydrocarbon accumulation (Wang et al., 2004a). Furthermore, the evaporites were deposited during Late Jurassic to Early Cretaceous time in the Tuonamu area with a total thickness of 31.0–188.4 m.
(2) Seismic exploration reveals that the subsalt traps were well developed in the Tuonamu area (Wang et al., 2009). Because the evaporites could serve as regional cap rocks, subsurface anticlines that formed under the subsalt overthrust zone are favorable habitats for giant oil and gas accumulations.
(3) The recognized micro-seepage anomalies display a string-bead-shaped pattern and some coincide with structure traps (Fig. 20a).
(4) The Tuonamu area is located in the margin of the central uplift. In the western part of this zone, a paleo-oil-reservoir and a large number of mud volcanoes (Fu et al., 2013) were discovered, indicating the occurrence of an active petroleum system.

4.2.2. Bandaohu area

The Bandaohu area is located in the middle part of the North Qiangtang depression covering an area about 1700 km^2 The tidal-lagoon shale, mudstone, and micritic limestone intercalated with gypsum salt in the Bailong Binghe Formation is a thick regional cap rock with a large thickness (>1161 m). The reservoirs consist of the Buqu Formation reef limestones, dolomites, and bioclastic limestones and the Suowa Formation reef limestones and bioclastic limestones. Source rocks are the Buqu Formation marls, Xiali Formation mudstones, and Bailong Binghe Formation shales and mudstones. The source rocks from the Buqu and Xiali Formations developed to a mature stage and began to expel petroleum plentifully in the Early Cretaceous, whereas the Bailong Binghe Formation source rock was still immature because of its shallow burial depth.

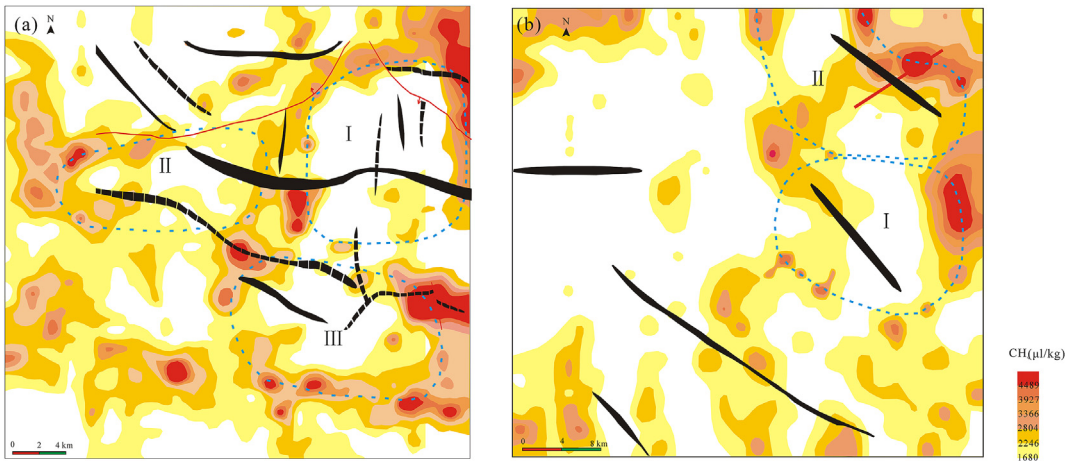

Fig. 20. Anomalies of acid-extractable CH_4 in the study area of the Qiangtang Basin. (a) Tuonamu area, (b) Bandaohu area.

Interpretation of seismic data (Wang et al., 2009) indicates that the Buqu Formation primary paleo-reservoirs (self-generating and self-storing) are widespread in the Bandaohu area. This area, with the Cenozoic strata directly overlain by the Bailong Binghe

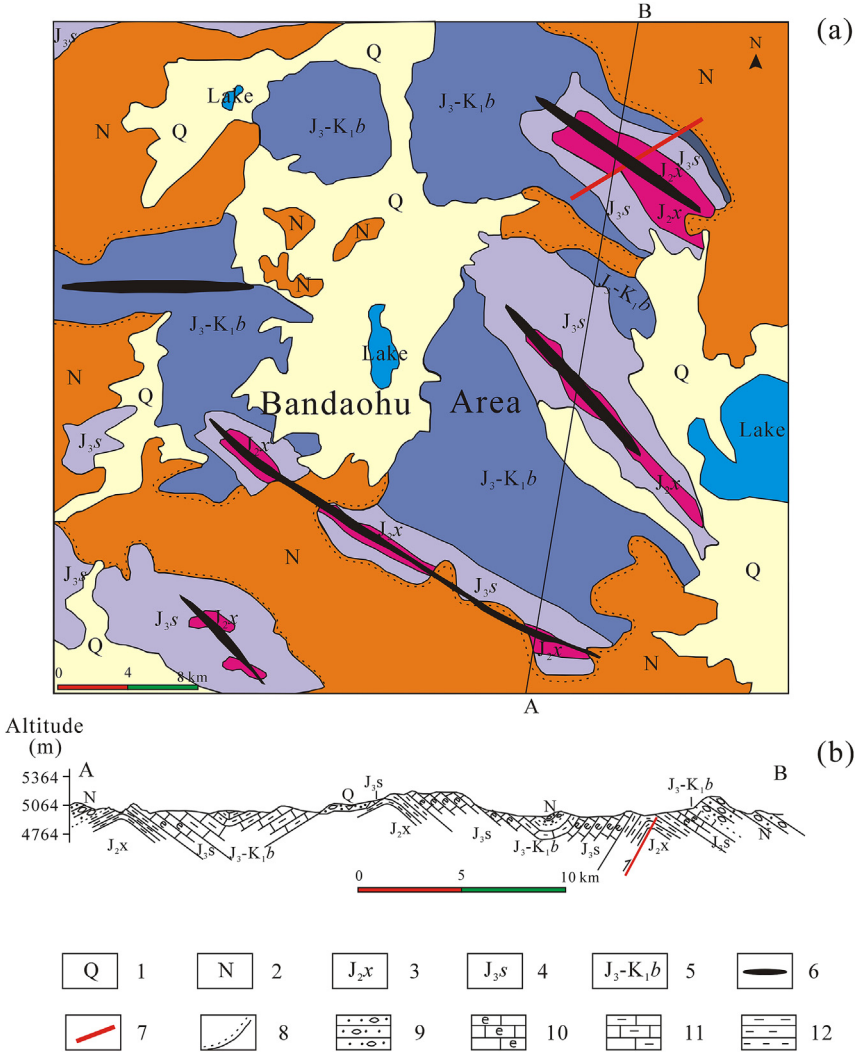

Fig. 21. Simplified tectonic map of the Bandaohu area in the Qiangtang Basin and schematic cross section (the location is in Fig. 15a) across this area (modified from Wang et al., 2009). 1, Quaternary; 2, Neogene; 3, Xiali Formation; 4, Suowa Formation; 5, Bailong Binghe Formation; 6, Anticline; 7, Fault; 8, Unconformity; 9, conglomerate; 10, Bioclastic limestone; 11; Marl; 12, Mudstone.

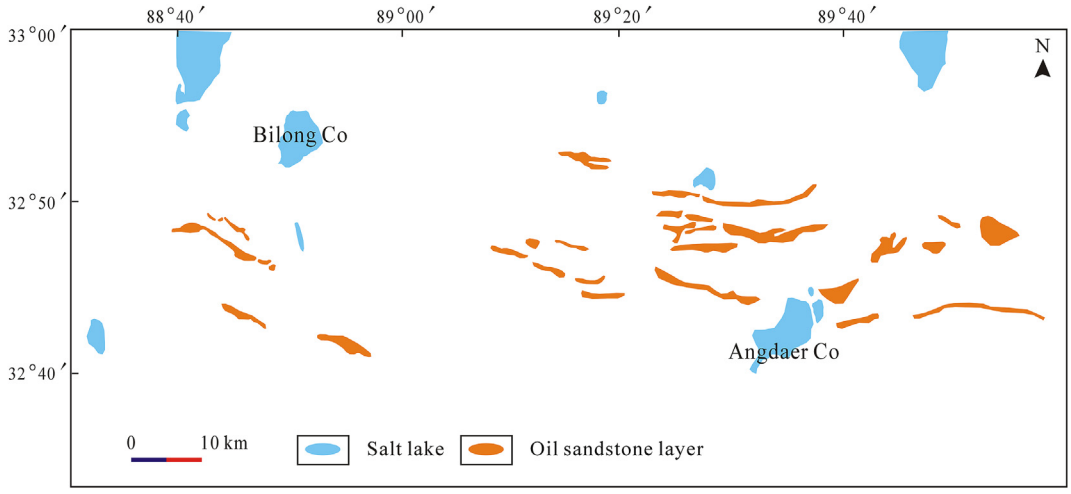

Fig. 22. Paleo-oil-reservoir zone found in the South Qiangtang depression.

Formation strata (Fig. 21), developed relatively abundant structural traps and suffered gentle structural transformation, resulting in partial destruction of the paleo-reservoirs; the residual petroleum probably migrated into the overlying strata along the faults.

Five large-scale anticlines are identified by geological survey (Fig. 21) and seismic interpretation (Wang et al., 2009) in the Bandaohu area, with areas ranging from 35 to 108 km^2 for each. Structural trap formation in the Bandaohu area occurred by the end of the Late Jurassic. Therefore, large-scale paleo-anticlines and lithological traps are favorable targets in the Bandaohu area.

Additionally, the Bandaohu area is considered to be one of the most favorable targets for oil and gas accumulation, owing to the following facts:

(1) There are excellent preservation conditions in the Bandaohu area. The tectonic movements were very weak in the Bandaohu area after hydrocarbon accumulation (Wang et al., 2004a), and the evaporites were also deposited during Late Jurassic to Early Cretaceous time with a total thickness of 13.0–64.4 m.
(2) Seismic exploration has revealed that the Jurassic reef traps were well developed in the Bandaohu area (Wang et al., 2009). The evaporites and marls could serve as the cap rocks of these traps, and the faults connect the reef traps to the source rocks.
(3) A Jurassic paleo-oil-reservoir zone had been discovered in the South Qiangtang depression, where the dolomite and reef are important reservoirs (Zhao and Li, 2000).
(4) The recognized micro-seepage anomalies also display a string-bead-shaped pattern and some are coincide with structure traps (Fig. 20b).

4.3. Hydrocarbon exploration potential and risk assessments

Wang et al. (2004a, 2009) proposed that the total oil resources in the hydrocarbon systems of the Qiangtang Basin amount to 10.43×10^9 t. Their study indicated that the North Qiangtang depression contains 6.08×10^9 t of these hydrocarbon resources, with 2.89×10^9 m^3 in the form of natural gas and 4.28×10^9 t in the form of oil (Wang et al., 2009). The South Qiangtang depression contains 4.35×10^9 t, including 2.73×10^9 t in the form of oil and 1.59×10^9 m^3 in the form of natural gas (Wang et al., 2009). It can be seen that the North Qiangtang depression should be delineated as the primary target for the purpose of oil and gas exploration.

Our studies revealed a large paleo-oil-reservoir zone (Fig. 22) in the South Qiangtang depression, covering an area of about 3000 km^2. The Buqu Formation dolomite is the main reservoirs in this zone, and also is the most important reservoirs in the basin as mentioned above. These dolomite reservoirs deposited in tidal flat environments. Tidal flat deposits were also developed in the North Qiangtang depression (e.g., the Bandaohu area), and show good preservation conditions as discussed above. These targets have a buried depth of 4000–5000 m. Therefore, tidal flat dolomites in the North Qiangtang depression are considered to have significant exploration potential.

Present petroleum exploration and development are centered mainly on the Mesozoic hydrocarbon systems. However, recent

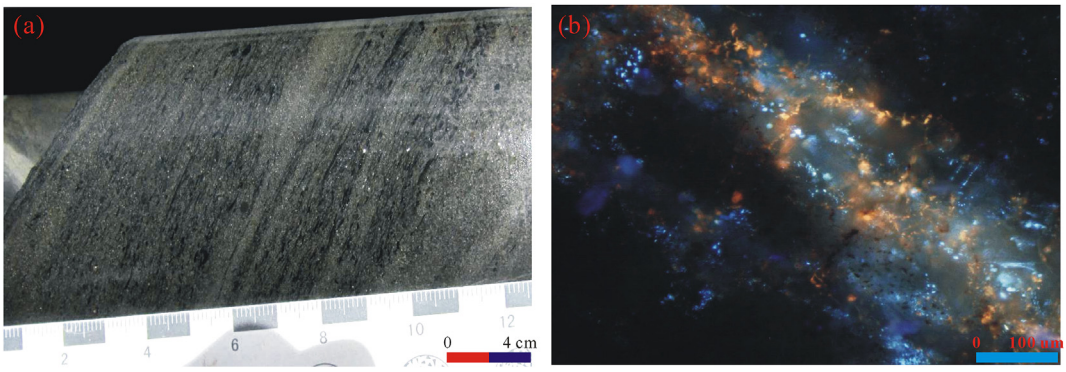

Fig. 23. Oil sandstone layer (a) and oil inclusions (b) in the Permian strata from the QZ-6 well.

investigations show that Paleozoic hydrocarbon systems are also considered to have significant exploration potential. For example, the Carboniferous Chameng Formation contains about 30.0–50.0 m of black shale with average TOC contents of 1.10%, and Ro in the range of 2.06–2.37% (Table 1, Supplementary Table 1), indicating a good potential for gas generation. Additionally, a Permian paleo-oil-reservoir was also discovered in the central uplift by shallow well investigation (QZ-6 well in Fig. 1). An oil sandstone layer (Fig. 23a) of about 50 m thick was penetrated in the QZ-6 well, and oil most likely derived from an underlying mudstone was trapped as abundant oil inclusions (Fig. 23b). Therefore, the Paleozoic hydrocarbon systems should be favorable targets for the future.

Present petroleum exploration has focused on the structural traps, and more than seventy potential anticlines are identified in the Qiangtang Basin. However, seal rupture due to late stage tectonics could be a risk for some potential structural traps. A further risk factor could be poor quality of source rocks of the Jurassic, which are the main exploration targets. As mentioned above, most of the Jurassic source rocks exhibit poor to fair quality as hydrocarbon source rocks. Although the Jurassic Xiali Formation mudstones are moderately-good source rocks, their distribution range is limited.

5. Conclusions

1. Several potential source rocks in the Qiangtang Basin, among which the coal-bearing mudstones of the Triassic Tumen Gela Formation are the best source rocks and the Jurassic Xiali Formation mudstones are moderately-good source rocks, while the Jurassic Buqu Formation and Suowa Formation carbonates exhibit poor to fair quality as hydrocarbon source rocks.
2. Middle Jurassic Buqu Formation dolomites are the main reservoirs in the basin. Additionally, pre-Nadi Kangri paleo-weathering crusts, Quemo Co Formation alluvial and fluvial sandstones, and Xiali Formation littoral sandstones are also potential reservoirs in the Qiangtang Basin.
3. The favorable areas were identified by studying the sedimentary facies, source rocks, reservoir rocks, cap rocks, traps, and preservation of oil and gas resources. Nine favorable hydrocarbon exploration areas were proposed in this paper, of which the Tuonamu area and Badaohu area are selected as the key targets for exploration for oil and gas resources in the basin.
4. The North Qiangtang depression should be delineated as the main target for the purpose of oil and gas exploration. Well-preserved dolomites in the Buqu Formation are considered to have significant exploration potential.

Acknowledgements

This work was jointly supported by the National Natural Science Foundation of China (No. 41172098, 40972087), the National Oil and Gas Special Project (No.XQ-2009-01), and the Qiangtang Basin gas hydrate resource exploration (No. GZHL20110301).

Appendix A. Supplementary data

Supplementary data related to this article can be found at http://dx.doi.org/10.1016/j.marpetgeo.2016.06.015.

References

Bishop, A.N., Love, G.D., Mcaulay, A.D., Snape, C.E., Farrimond, P., 1998. Release of kerogen-bound hopanoids by hydropyrolysis. Org. Geochem 29, 989–1001.
Chen, L., Yi, H.S., Hu, R.Z., Zhong, H., Zou, Y.R., 2005. Organic geochemistry of the Early Jurassic oil shale from the Shuanghu area in northern Tibet and the Early Toarcian oceanic anoxic event. Acta Geol. Sin. Engl. 79, 392–397.
Chengdu Institute of Geology and Mineral Resources, 2005a. Regional Geological Report (1:250,000) for Heihuling, P.R.C, pp. 23–88 (in Chinese).
Chengdu Institute of Geology and Mineral Resources, 2005b. Regional Geological Report (1:250,000) for Jiangaidarina, P.R.C, pp. 200–205 (in Chinese).
Delbrouck, O., Janssen, J., Ottenburgs, R., Oyen, P.V., Viaene, W., 1993. Evolution of porosity in extruded stoneware as a function of firing temperature. Appl. Clay Sci. 8, 187–192.
Dewey, J.F., Shackleton, R.M., Chang, C., Yi, Y.S., 1988. The tectonic evolution of the Tibetan Plateau. Philos. Trans. Roy. Soc. Lond. Ser. A 327, 379–413.
Ding, W.L., Wan, H., Su, A.G., He, Z.H., 2011. Characteristics of Triassic marine source rocks and prediction of favorable source kitchens in Qiangtang Basin. Tibet. Energy Explor. Exploit. 29, 143–160.
Fu, X.G., Liao, Z.L., Wang, J., Chen, W.B., 2008. Geochemistry and significance of oil seepage in the Zaring area of the southern Qiangtang depression, northern Tibet. Acta sedment. Sin. 26, 697–704 (in Chinese with English abstract).
Fu, X.G., Wang, J., Wu, T., He, J.L., 2009. Discovery of the large-sacale paleo-weathering crust in the Qiangtang Basin, northern Tibet, China and its significance. Geol. Bull. China 28, 696–700 (in Chinese with English abstract).
Fu, X.G., Wang, J., Tan, F.W., Chen, M., Chen, W.B., 2010a. The Late Triassic rift-related volcanic rocks from eastern Qiangtang, northern Tibet (China): age and tectonic implications. Gondwana Res. 17, 135–144.
Fu, X.G., Wang, J., Wu, T., He, J.L., 2010b. Stratigraphy and paleoenvironment of the Quemo Co formation in Shengli river area, northern Tibet (in Chinese). Geol. China 37, 1305–1312 (in Chinese with English abstract).
Fu, X.G., Wang, J., Tan, F.W., Feng, X.L., Wang, D., He, J.L., 2013. Gas hydrate formation and accumulation potential in the Qiangtang Basin, northern Tibet, China. Energy Convers. Manage 73, 186–194.
He, J.L., Wang, J., Tan, F.W., Chen, M., Li, Z.X., Sun, T., Wang, P.K., Du, B.W., Chen, W.B., 2014. A comparative study between present and palaeo-heat flow in the Qiangtang Basin, northern Tibet, China. Mar. Pet.. Geol. 57, 345–358.
Kapp, P., Yin, A., Manning, C.E., Harrison, T.K., Taylor, M.H., Ding, L., 2003. Tectonic evolution of the early Mesozoic blueschist-bearing Qiangtang metermorphic belt, central Tibet. Tectonics 22. http://dx.doi.org/10.1029/2002TC001383.
Klemme, H., Ulmishek, G., 1991. Effective petroleum source rocks of the world-stratigraphic distribution and controlling depositional factors. AAPG Bull. 75, 1809–1851.
Liang, X., Wang, G.H., Yuan, G.L., Liu, Y., 2012. Structural sequence and geochronology of the Qomo Ri accretionary complex, central Qiangtang, Tibet: implications for the late Triassic subduction of the paleo-Tethys ocean. Gondwana Res. 22, 470–481.
Nie, S., Yin, A., Rowley, D.B., Jin, Y., 1994. Exhumation of the Dabie Shan ulrea-high pressure rocks and accumulation of the Songpan-Ganzi flysch sequence, central China. Geology 22, 999–1002.
Pearce, J.A., Mei, H., 1988. Volcanic rocks of the 1985 Tibet Geotraverse: Lhasa to Golmud. Philos. Trans. Roy. Soc. Lond. Ser. A 327, 169–201.
Sun, Z.J., Yang, Z.B., Mei, H., Qin, A.H., Zhang, F.G., Zhou, Y.L., Zhang, S.Y., Mei, B.W., 2014. Geochemical characteristics of the shallow soil above the Muli gas hydrate reservoir in the permafrost region of the Qilian Mountains, China. J. Geochem. Explor 139, 160–169.
Wang, C.S., Yi, H.S., Liu, C.Y., Li, Y.L., Zou, Y.R., Wu, X.H., Deng, B., Yang, X.K., 2004b. Discovery of paleo-oil-reservoir in Qiangtang Basin in Tibet and its geological significance. Oil Gas Geol. 25, 139–143 (in Chinese with English abstract).
Wang, J., Tan, F.W., Li, Y.L., Li, Y.T., Chen, M., Wang, C.S., Guo, Z.J., Wang, X.L., Du, B.W., Zhu, Z.F., 2004a. The Potential of the Oil and Gas Resources in Major Sedimentary Basins on the Qinghai-xizang Plateau (in Chinese). Geological Publishing House, Beijing, pp. 34–88 (in Chinese with English abstract).
Wang, J., Ding, J., Wang, C.S., Tan, F.W., Chen, M., Hu, P., Li, Y.L., Gao, R., Fang, H., Zhu, L.D., Li, Q.S., Zhang, M.H., Du, B.W., Fu, X.G., Li, Z.X., Wan, F., 2009. Survey and Evaluation on Tibet Oil and Gas Resources (in Chinese). Geological Publishing House, Beijing, pp. 11–223 (in Chinese).
Xiong, B., Li, X.Q., Li, Y.B., Tan, Q., 2009. The surface geochemical exploration of oil and gas in the Gangbatong-Ya'anxiang and the Dongqiao-Nam Co of the Qinghai-Tibet region. Sci. China Earth Sci. 52, 69–76.
Yang, M.Y., Jeon, C.W., Yang, M.K., Lee, S.H., Wakita, H., 1997. Analysis of the organic matter in oil shales distributed in Korea. Anal. Sci. 13, 433–436.
Yeomans, J., Bremmer, J.M., 1989. A rapid and precise method four routine determination of organic carbon in soil. Comm. Soil Sci. Plant Anal. 19, 1467–1476.
Yin, A., Harrison, T.M., 2000. Geologic evolution of the Himalayan-Tibetan Orogen. Annu. Rev. Earth Plant Sci. 28, 211–280.
Zeng, Y.H., Fu, X.G., Zeng, S.Q., Du, G., 2013. Upper Triassic potential source rocks in the Qiangtang Basin, Tibet: organic geochemical characteristics. J. Pet.. Geol. 36, 237–255.
Zhang, H.R., Yang, T.N., Hou, Z.Q., Song, Y.C., Ding, Y., Cheng, X.F., 2013. Petrogenesis and tectonics of late Permian felsic volcanic rocks, eastern Qiangtang block, north-central Tibet: Sr and Nd isotopic evidence. Int. Geol. Rev. 55, 1017–1028.
Zhao, Z.Z., Li, Y.T., 2000. Conditions of petroleum geology of the Qiangtang Basin of the Qinghai-Tibet plateau. Acta Geol. Sin. - Engl. 74, 661–665.
Zhao, Z.Z., Li, Y.T., Ye, H.F., Zhang, Y.W., 2000. Oil and Gas Generation of Mesozoic Marine Source Rock in the Qinghai-xizang Plateau, China. Science Press, Beijing, p. 214 (in Chinese).